

LIBRARY Michigan State University

This is to certify that the

thesis entitled

The Effect of Halogen Ion Substitution on the Superconducting Properties of Y-Ba-Cu-Oxygen System presented by

Jaimoo Yoo

has been accepted towards fulfillment of the requirements for

Master's degree in Material Science

Date February 16, 1990

جر ۽

PLACE IN RETURN BOX to remove this checkout from your record. TO AVOID FINES return on or before date due.

DATE DUE	DATE DUE	DATE DUE
	-	

MSU is An Affirmative Action/Equal Opportunity Institution ctoircidatedua.pm3-p.

# THE EFFECT OF HALOGEN ION SUBSTITUTION ON THE SUPERCONDUCTING PROPERTIES OF Y-Ba-Cu-Oxygen SYSTEM

By

Jaimoo Yoo

## A THESIS

Submitted to
Michigan State University
in partial fullfillment of the requirements
for the degree of

# MASTER OF SCIENCE

Department of Metallurgy, Mechanics, and Materials Science

#### ABSTRACT

THE EFFECT OF HALOGEN ION SUBSTITUTION ON THE SUPERCONDUCTING PROPERTIES OF Y-Ba-Cu-Oxygen SYSTEM

Ву

Jaimoo Yoo

Since the discovery of high critical temperature in the Y-Ba-Cu-O compound, a number of investigators have suggested that the critical temperature of this compound can be in creased by halogen ion, such as F and Cl, additions.

These results still remain controversial. At Michigan State University, a systematic study was undertaken to investigate and evaluate iodine ion substitution in this system by using CuI as iodine agent. It was found that the iodine substituted compounds of Y-Ba-Cu-O had a critical temperature of 100K and an onset temperature of 110K. A small amount of iodine was detected by EDAX analysis. In this thesis, method of sample preparation, optimum composition and electrical properties of these compounds are presented. Also discussed are microstructural aspects of this high temperature superconductor.

#### **ACKNOLEDGEMENTS**

I would like to express my most sincere thanks to Dr.

K. Mukherjee and my parents for their constant support

and guidance during this research. I would like to thank Dr.

P.A.A. Khan for his valuable suggestions. I like to express

personal appreciation to my lovely wife Jungsook Kim for

her never ending love and encouragement. I would also like to

thank Mr. S.H. Nam, Mr. C.S. Kim, Mr. G.E. Jang, Mr. I.S. Oh

and Mr. C.W. Chen for their timely help and support.

# TABLE OF CONTENTS

			Page
LIST	OF	FIGURES	v
LIST	OF	TABLES	vii
1.	INT	RODUCTION	1
2.	LITI	ERATURE SURVEY	
	2-1	Crystal Structure of Y-Ba-Cu-O Compound	4
	2-2	Anisotropy Nature of Y-Ba-Cu-O Compound	7
	2-3	Substitution of Cu with 3-d Metal in Y-Ba-Cu-O Compound	10
	2-4	Fluorine Controversy	14
3.	EXP	ERIMENTAL PROCEDURE	
	3-1	Sample Preparation	20
	3-2	Magnetic Separation and Sintering	21
	3-3	Critical Temperature Measurement Set-Up	24
	3-4	Critical Current Density Measurement Set-Up	30
	3-5	EDAX and X-Ray Diffraction	33
	3-6	Morphological Examination	
		3-6-1 Electron Microscopy	34
		3-6-2 Optical Microscopy	34
4.	RESU	JLT AND DISCUSSION	
	4-1	Critical Temperature Measurement	35
	4-2	Critical Current Density Measurement	39
	4-3	EDAX and X-Ray Analysis	42
	4-4	Microstructure of Iodine Substituted 1:2:3 Sample	50

5.	CONCLUSIONS	56
6.	REFERENCES	57

### LIST OF FIGURES

Figure	Page
<ol> <li>Crystal structure of YBa<sub>2</sub>Cu<sub>3</sub>O<sub>7-X</sub>.</li> <li>Dashed circles represent vacant sites (Ref. 16)</li> </ol>	6
2. Magnetization hysteresis loops at 4.5K for a single crystal of 1:2:3 with the Cu-O planes oriented (a) perpendicular to the magnetic field and (b) parallel to the applied field (Ref. 17)	8
3. Critical current densities deduced from magnetization hysteresis as a function of magnetic field applied either parallel or perpendicular to the Cu-O planes (Ref. 17)	9
4. Temperature dependence of the normalized resistance of YBa <sub>2</sub> Cu(Cu <sub>0.9</sub> A <sub>0.1</sub> ) <sub>3</sub> O <sub>6+2</sub> , where A = Cr, Mn, Fe, Co, Ni and Zn (Ref. 5)	11
5. Resistance vs temperature measurement of nominal composition YBa <sub>2</sub> Cu <sub>3</sub> F <sub>2</sub> O <sub>2</sub> . Curve A shows the resistance upon initial cooling; curve B, data obtained upon second cooling; and curve C, data from warming after second cooling (Ref. 7)	15
<ol> <li>Powder x-ray diffraction patterns of fluoride doped samples of YBa<sub>2</sub>Cu<sub>3</sub>F<sub>x</sub>O<sub>2</sub>.</li> <li>Value of X: (a) 0.0165, (b) 0.066 (c) 0.825 (d) 1.65 (Ref. 8)</li> </ol>	17
<ol> <li>Schematic diagram of the magnetic separation procedure. (a) Before doing magnetic separation (b) Under moving magnet</li> </ol>	22
8. Schematic of 4 wire AC resistance measurement	25
9. Schematic of (a) 4 gold plated wire (b) with superconducting sample	26
10. Sample holder assembly for 4 contact direct AC resistance measurement	27
11. Schematic diagram of resistance measurement	

	set-up	29
12.	Schematic diagram of $J_c$ measurement set-up	31
13.	Temperature effect on resistance of $YBa_2Cu_3I_xO_z$ (X=1,2,3), where $I_1$ represents $YBa_2Cu_3I_1O_{5.5}$ etc	36
14.	The cooling and heating cyclic measurement of the resistance of $YBa_2Cu_3I_1O_{5.5}$	38
15.	Current-voltage curve of YBa <sub>2</sub> Cu <sub>3</sub> I <sub>1</sub> O <sub>5.5</sub>	40
16.	The EDAX spectra of YBa <sub>2</sub> Cu <sub>3</sub> I <sub>1</sub> O <sub>5.5</sub> sample	43
17.	The EDAX spectra of YBa2Cu3I2O4.5 sample	44
18.	The EDAX spectra of YBa <sub>2</sub> Cu <sub>3</sub> I <sub>3</sub> O <sub>3.5</sub> sample	45
19.	X-ray diffraction patterns of a) 1:2:3 sample b) YBa <sub>2</sub> Cu <sub>3</sub> I <sub>1</sub> O <sub>5.5</sub> sample	46
20.	X-ray diffraction patterns of YBa <sub>2</sub> Cu <sub>3</sub> I <sub>2</sub> O <sub>4.5</sub> sample	48
21.	X-ray diffraction patterns of YBa <sub>2</sub> Cu <sub>3</sub> I <sub>3</sub> O <sub>3.5</sub> sample	49
22.	Optical microscopy of YBa <sub>2</sub> Cu <sub>3</sub> I <sub>1</sub> O <sub>5.5</sub>	51
23.	Optical microscopy of a) YBa <sub>2</sub> Cu <sub>3</sub> I <sub>2</sub> O <sub>4.5</sub> b) YBa <sub>2</sub> Cu <sub>3</sub> I <sub>3</sub> O <sub>3.5</sub>	52
24.	SEM micrograph of YBa <sub>2</sub> Cu <sub>3</sub> I <sub>1</sub> O <sub>5.5</sub>	53
25.	SEM micrograph of a) YBa <sub>2</sub> Cu <sub>3</sub> I <sub>2</sub> O <sub>4.5</sub> b) YBa <sub>2</sub> Cu <sub>3</sub> I <sub>3</sub> O <sub>3.5</sub>	54

# LIST OF TABLES

Tal	Table Table	
1.	T <sub>c</sub> , Measured Susceptibility at 100K and Calculated Values of Magnetic Moment (Ref. 5)	13
	(Rel. 3)	13
2.	Phase Distribution in Samples with Nominal Compositions of $YBa_2Cu_3F_XCl_YO_Z$ (Ref. 9)	16
3.	Critical Temperature and Transition Width of Composition of $YBa_2Cu_3F_XO_Z$ (Ref. 8)	18
4.	The Superconductivity Data of Nominal YBa <sub>2</sub> Cu <sub>3</sub> F <sub>x</sub> Cl <sub>y</sub> O <sub>2</sub> (Ref. 9)	18

#### 1. INTRODUCTION

In 1987, Wu et al. [1] first found a high critical temperature ( $T_c = 90$  to 95K) superconductor, based upon the replacement of La by Y of a RBa<sub>2</sub>Cu<sub>3</sub>O<sub>7</sub> (R represents rare earth material). This has generated widespread experimental and theoretical research work related with high values of  $T_c$ . A number of researchers have tried various element substitutions in Y-Ba-Cu-O compound, to further increase the critical temperature. Substitution in Y sites of Y-Ba-Cu-O compound by rare earth elements, such as Gd, or substitution of Ba with Sr, do not affect critical temperature [2,3], because, the rare earth element sites and Ba sites are not much involved in superconductivity of Y-Ba-Cu-O compound.

Several authors have reported that substitution of Cu with 3-d transition metals such as Ni, Zn or Co can sharply reduce critical temperature [4,5,6]. A clear explanation of why reduction in  $T_c$  takes place when substitutions are made for Cu, was not provided.

Recently, it was reported that fluorine substituted Y-Ba-Cu-O compound has a very high critical temperature [7] (up to 155K). Other researchers, however do not support the claim that higher critical temperature is obtained by F or Cl substitution [8,9]. Narottam et al.[8] reported that critical temperature was slightly increased and the transition behavior was sharpened with low fluorine concentra-

tions. Other paper which investigated fluorinated and chlorinated Y-Ba-Cu-O compound, using  $BaF_2$  and  $BaCl_2$  as the fluorination and chlorination agents, reported no such increase in  $T_c$ . To the contrary, they reported that higher substitution levels of fluorine and chlorine sharply decreased  $T_c$  [9].

In the present study, a systematic investigation was undertaken to evaluate the effects of iodine ion substitution in Y-Ba-Cu-O compound. In this study, CuI is used as the iodine agent. Copper iodide was selected, for addition to Y-Ba-Cu-O compound, because of the following reasons:

- 1. Among the halogen elements, iodine has the highest diamagnetic susceptibility and thus it was speculated that this element might contribute to the net diamagnetism associated with the superconducting phase.
- 2. Copper source originated from the dissociation of CuI is available to form Cu-O chain which is important for superconductivity.
- 3. The melting and boiling temperatures of CuI are such that at the sintering temperature of the superconducting oxide, no adverse effect is produced.

In this investigation, The critical temperature and current density were measured by using a standard four point technique and optical and scanning electron microscopes were used to study microstructural aspects of this high temperature superconductor. Furthermore, EDAX analysis was used to

determine the presence of iodine in 1:2:3 superconducting compound in which various proportions of CuI were added.

#### 2. LITERATURE SURVEY

# 2-1 Crystal Structure of Y-Ba-Cu-O Compound

Though the structure of Y-Ba-Cu-O compound, based on x-ray diffraction and neutron diffraction studies, is well documented [10-14], the mechanism of conductivity in high critical temperature superconductors is not yet clearly understood. The superconducting phase YBa<sub>2</sub>Cu<sub>3</sub>O<sub>7-X</sub> (subscript X represent unknown oxygen content) is an orthorhombic, oxygen deficient, perovskite like structure which can be visualized as a stack of alternating perovskite structures: (BaCuO<sub>3</sub>): (YCuO<sub>3</sub>): (BaCuO<sub>3</sub>) [14,15]. Compounds with the perovskite structure have the formula of ABO<sub>3</sub>, where A is the relatively large ion in the center of unit cell, B is a small ion at the corners and O is the oxygen ions at the edge of the unit cell [15].

However, there are some differences between Y-Ba-Cu-O structure and the three stacked perovskite structure as mentioned above. In a perovskite structure, copper ions are located in the center of an oxygen octahedron. In YBa<sub>2</sub>Cu<sub>3</sub>O<sub>7-X</sub> structure, copper ions occupy two symmetry sites [13,16]. Copper ions are located in approximately the (003) plane and have five oxygen neighbors due to the vacancies of oxygen atom in the (002) yttrium atom plane. The Cu-O polyhedron is a square pyramid with the copper ion positioned slightly

above the Cu plane as shown in Fig. 1. Copper ions in the basal plane have only four oxygen atoms due to the vacancies of oxygen atom in the basal plane.

Fig. 1 presents the Y-Ba-Cu-O crystal structure determined by neutron diffraction and x-ray studies [10-14]. Unit cell dimensions for this structure at room temperature are a=3.8187Å, b=3.8833Å, c=11.6687Å [13]. In the (002) yttrium atom plane, all oxygen sites are vacant. In the basal plane, the vacancies of oxygen atom along the a axis lead to an orthorhombic deformation (a<b=c/3).

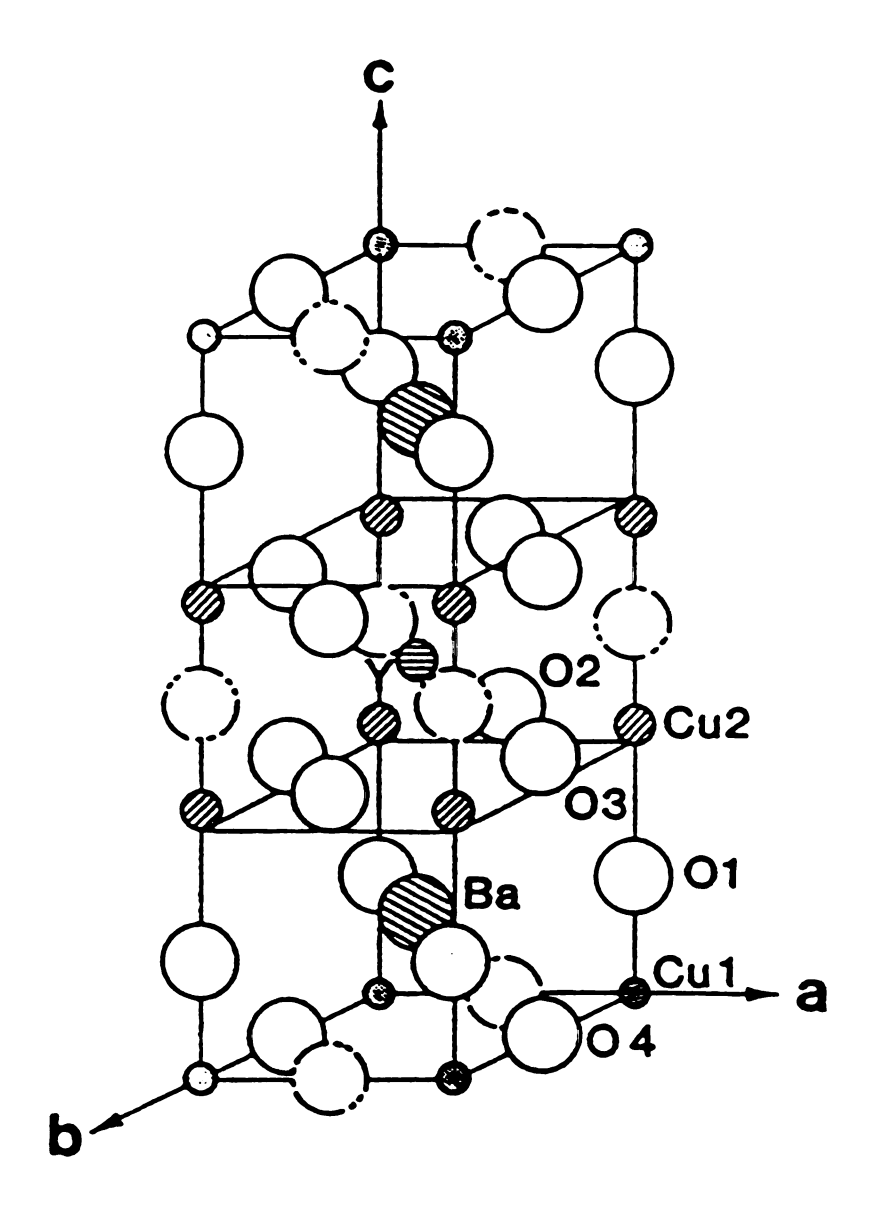


Fig. 1. Crystal structure of YBa<sub>2</sub>Cu<sub>3</sub>O<sub>7-X</sub>.

Dashed circles represent vacant sites (Ref. 16).

The anisotropic behavior of single crystal YBa<sub>2</sub>Cu<sub>3</sub>O<sub>7-X</sub> has been studied by magnetization of the crystal with the field applied both parallel and perpendicular to the Cu-O planes by several investigators [17,18].

Fig. 2 shows magnetic hysterisis loops at 4.5K for the Cu-O plane perpendicular to the field lines [Fig. 2(a)] and parallel to the field lines [Fig. 2(b)] [17]. In Fig. 2(a), actually the induced screening currents flow parallel to the Cu-O plane. Fig. 3 shows the field and temperature dependence of the critical current density determined from the hysterisis curves in Fig. 2. At low temperatures, in fields up to about 40KG, critical currents along the directions of Cu-O planes were in excess of 10<sup>6</sup> A/cm<sup>2</sup> [17]. These critical current and critical field measurements of 1:2:3 single crystals demonstrate a strong anisotrpy with the good conducting directions being along the Cu-O planes which is also supported by other papers [19,20]. Chaudhuri et al. first reported that high critical current density in excess of 105 A/cm<sup>2</sup> was found in epitaxially grown films of YBa<sub>2</sub>Cu<sub>3</sub>O<sub>7</sub> with c axis primary perpendicular to the plane of the film [21]. The current was flowing in the Cu-O plane. This practical application and magnetization of 1:2:3 single crystal measurements revealed strong anisotropy in critical current by a factor of about 10.

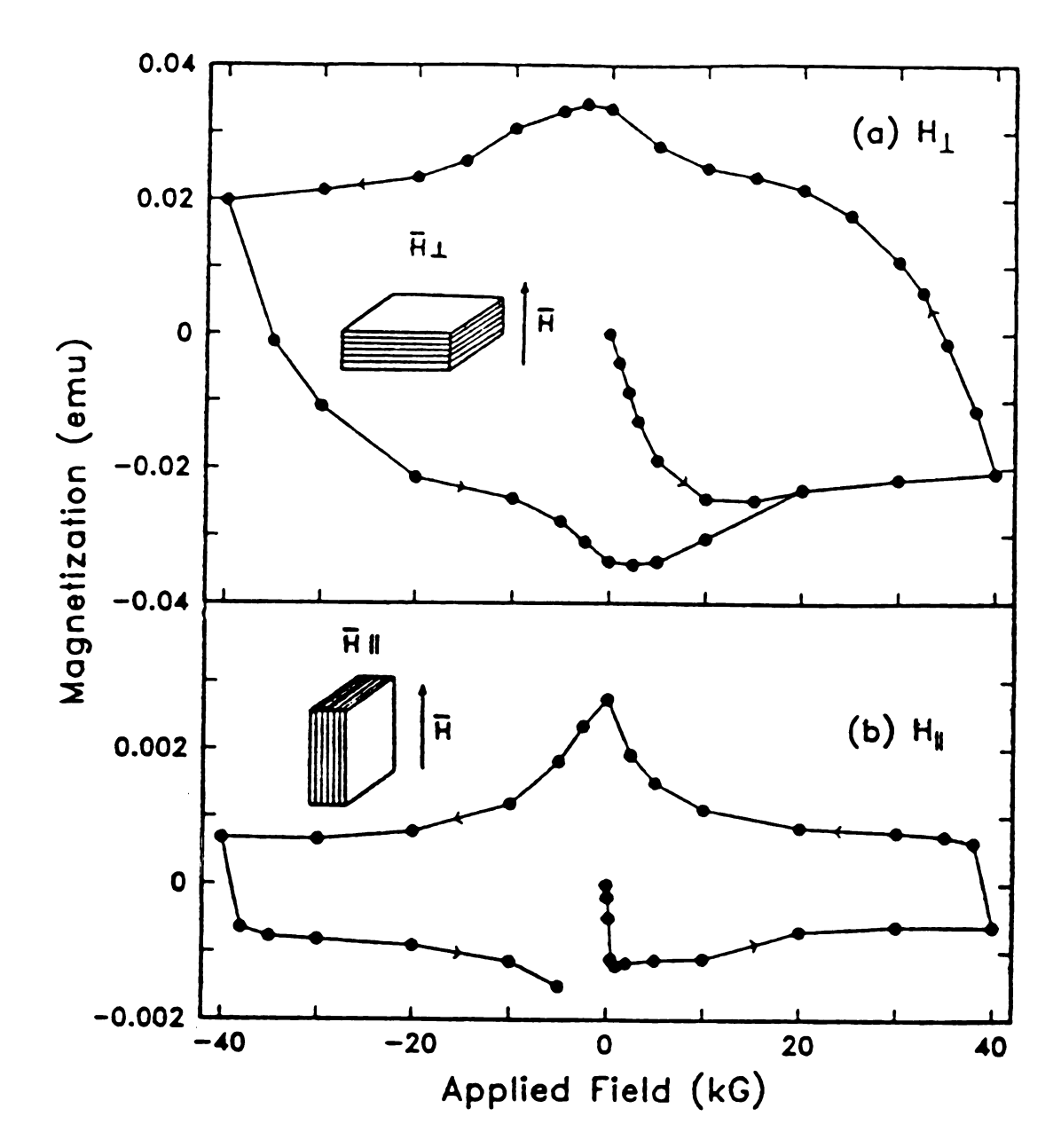


Fig. 2. Magnetization hysteresis loops at 4.5K for a single crystal of 1:2:3 with the Cu-O planes oriented (a) perpendicular to the magnetic field and (b) parallel to the applied field (Ref. 17).

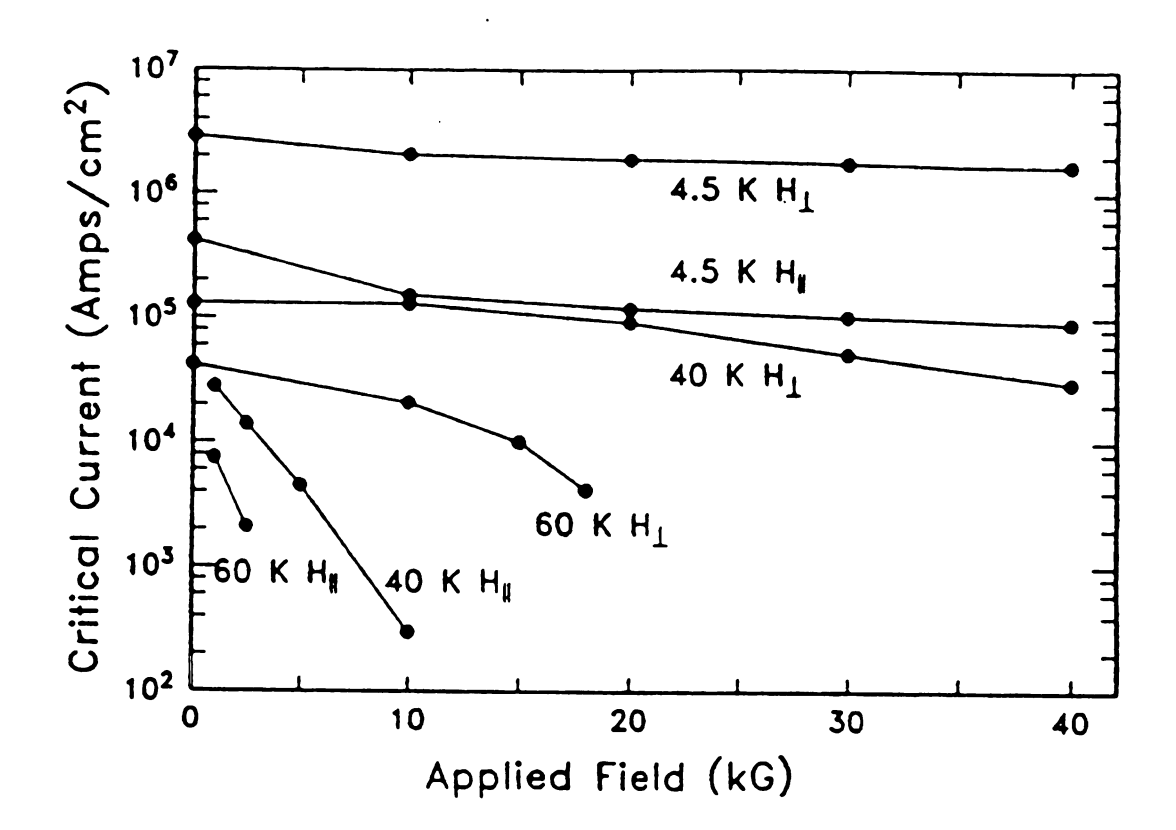


Fig. 3. Critical current densities deduced from magnetization hysteresis as a function of magnetic field applied either parallel or perpendicular to the Cu-O planes (Ref. 17).

# 2-3 Substitution of Cu with 3-d Metals in Y-Ba-Cu-O Compound

Many investigators [13,17,18] have implied that Cu-O chain is essential for the high temperature superconductivity. Thus, the effect of replacement of Cu with 3-d transition metals, could produce a substantial change in superconducting properties.

The superconducting properties of the mixed compound  $YBa_2(Cu_{3-x}A_x)O_{6+z}$ , where A=Ti, Cr, Mn, Fe, Co, Ni, Zn and Z=unknown oxygen contents, were investigated by several researchers [4,5,6]. The ionic size and orbital structure of the 3-d transition metal are close to those of Cu; they expected that 3-d transition metal will occupy the Cu sites if transition metal are substituted into 1:2:3 structure. Fig. 4 shows the temperature dependence of the normalized resistance for several samples. Substitutions by 3-d transition metals produce a reduction in  $T_c$  which is dependent on the substituted elements. It can be seen that for A=Ni, Fe, Co, Zn, the behavior is semiconductor like and the conduction electrons appear to become weakly localized before superconductivity starts [5].

 $T_c$  drops very sharply as 10% of the Cu is substituted by Zn as shown in Fig. 4. Gang Xiao et al. [5] proposed a possible explanation. The divalent Zn ions have ten 3-d electrons and thus the 3-d state is very stable, compared with the divalent Cu ion which has 9 electrons. Substitution

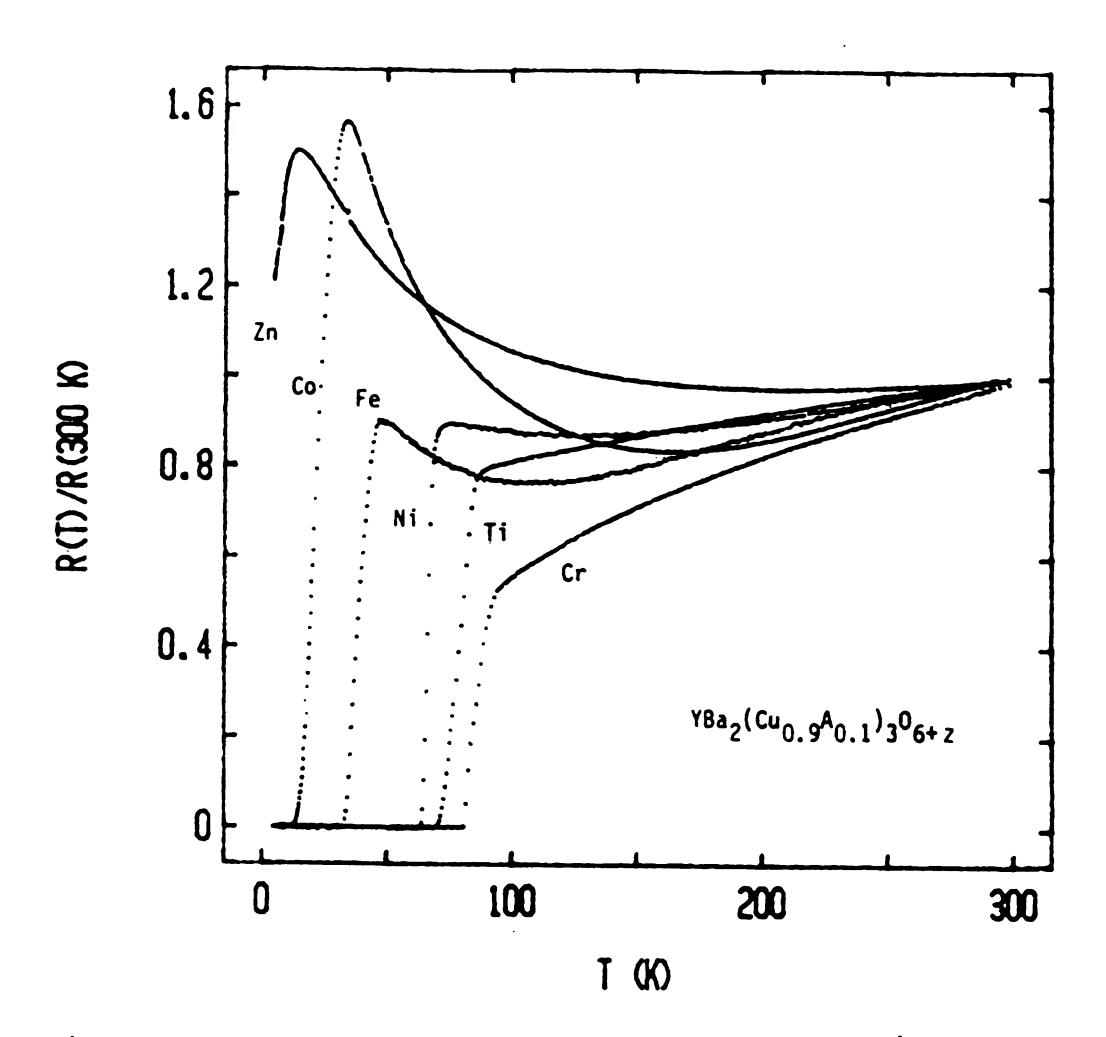


Fig. 4. Temperature dependence of the normalized resistance of  $YBa_2(Cu_{0.9}A_{0.1})_3O_{6+2}$ , where A = Cr, Mn, Fe, Co, Ni, and Zn (Ref. 5).

of Cu by Zn provides an extra electron which fills up antibonding d band and reduces the density of states  $(E_f)$  at those sites [5]. Tarascon et al. have suggested four interrelated explanations; structural disorder, oxygen vacancy, the dopants inducing a different oxidation state in the copper and magnetic depairing, for the reduction of  $T_c$  with 3-d metal substitution in the Cu-O planes [4].

Though a clear explanation is not available yet, it is generally believed, from the Arbrikosov and Gorkov theory [4], that the direct interactions of magnetic ions with the superconducting electrons breaks the cooper pairs and reduces critical temperature. The reduction relation between T<sub>c</sub> and magnetic impurity concentration looks like coincedence with Arbrikosov and Gorkov's theory qualitatively and large local paramagnetic moment in the mid 3-d elements as shown in Table 1 prefers magnetic depairing [5].

However, the supression of  $T_c$  due to magnetic scattering in this class of metals is not systematic. Especially,  $T_c$  reduction effect for substitution of Cu with Co is larger than that of Fe, eventhough the magnetic moment of Fe is larger than that of Co.

Table 1  $T_{\rm C}$ , Measured Susceptibility at 100K and Calculated Values of Magnetic Moment (Ref. 5)

A =	<i>T<sub>c</sub></i> (K)	χ <sub>exp</sub> (100 K) ×10 <sup>3</sup> emu/mol	PA
Ti	75.0	0.419	0-0.45
Cr	84.5	0 <b>.9</b> 88	≈0
Mn	78.9	1.821	1.35-2.01
Fe	38.0	5.004	3.29-3.61
Co	21.2	4.735	2.87-3.20
Ni	66.3	1.923	1.40-2.05
Cu	94.1	0.490	0.22
Zn	< 3.0	1.378	0.49*

## 2-4 Fluorine Controversy

There are many reports of critical temperature above 150K in Y-Ba-Cu-O compound [22,23]. Ovshinsky et al. claimed superconductivity at 155K for the first time in bulk 1:2:3 material [7]. They fabricated five element compound YBa<sub>2</sub>Cu<sub>3</sub>F<sub>X</sub>O<sub>2</sub> (subscript Z represent unknown oxygen contents) by substituting part of oxygen with fluorine. The temperature dependence of the resistance of a portion of X=2 sample is shown in Fig. 5. During heating and cooling (cyclic) measurements, the critical temperature was reported to vary between 168K -148K.

However, Yan et al., who investigated fluorinared 1:2:3 sample, reported that they didn't find such a high critical temperature [9]. Table 2 shows crystalline phase distribution in the sintered composition as observed by them [9]. The concentration of the YBa<sub>2</sub>Cu<sub>3</sub>O<sub>7</sub> superconducting phase, in the fluorinated samples, decreased with nominal fluorine concentration. This data is consistent with X-ray diffraction measurements for fluorinated 1:2:3 materials as reported by Narottam et al. [8] and shown in Fig. 6. From Fig. 6, it can be seen that samples with  $X \le 0.066$  contain nearly 100% superconducting orthorhombic perovskite phase. However, compositions with  $X \ge 0.165$  are multiphase, and consist of BaF<sub>2</sub>, CuO, and other unknown phases in addition to the superconducting perovskite phase [8]. From Table 2,

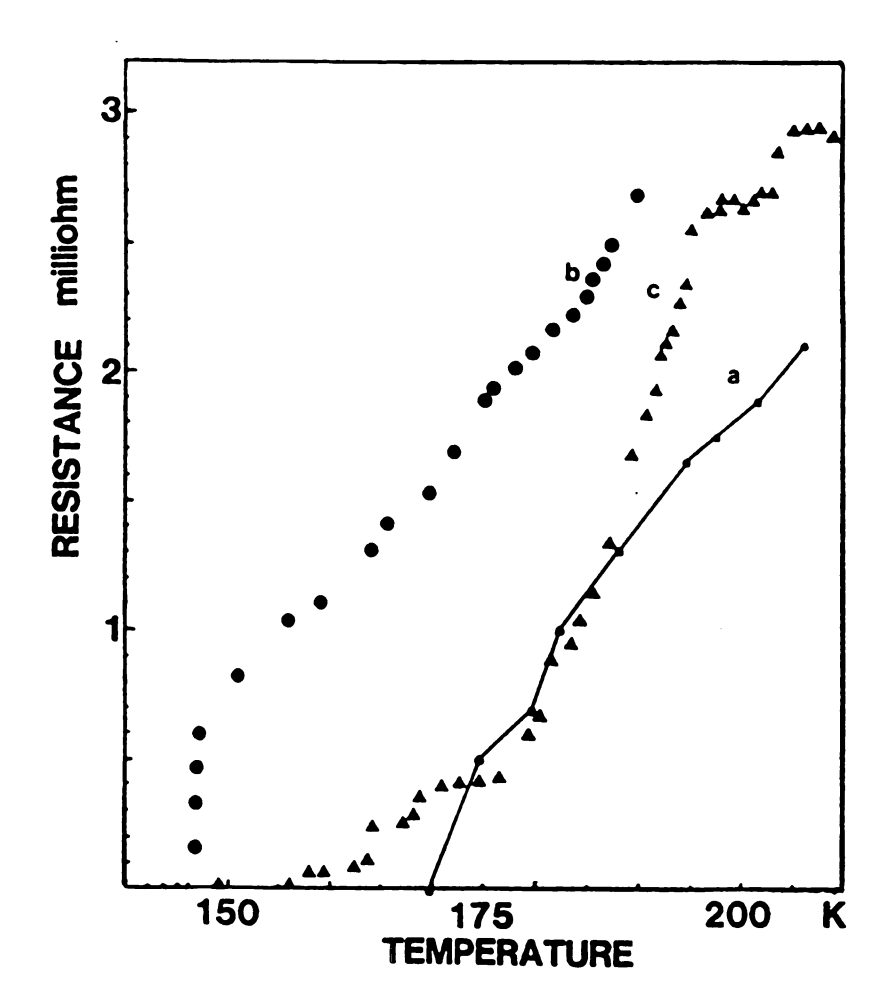
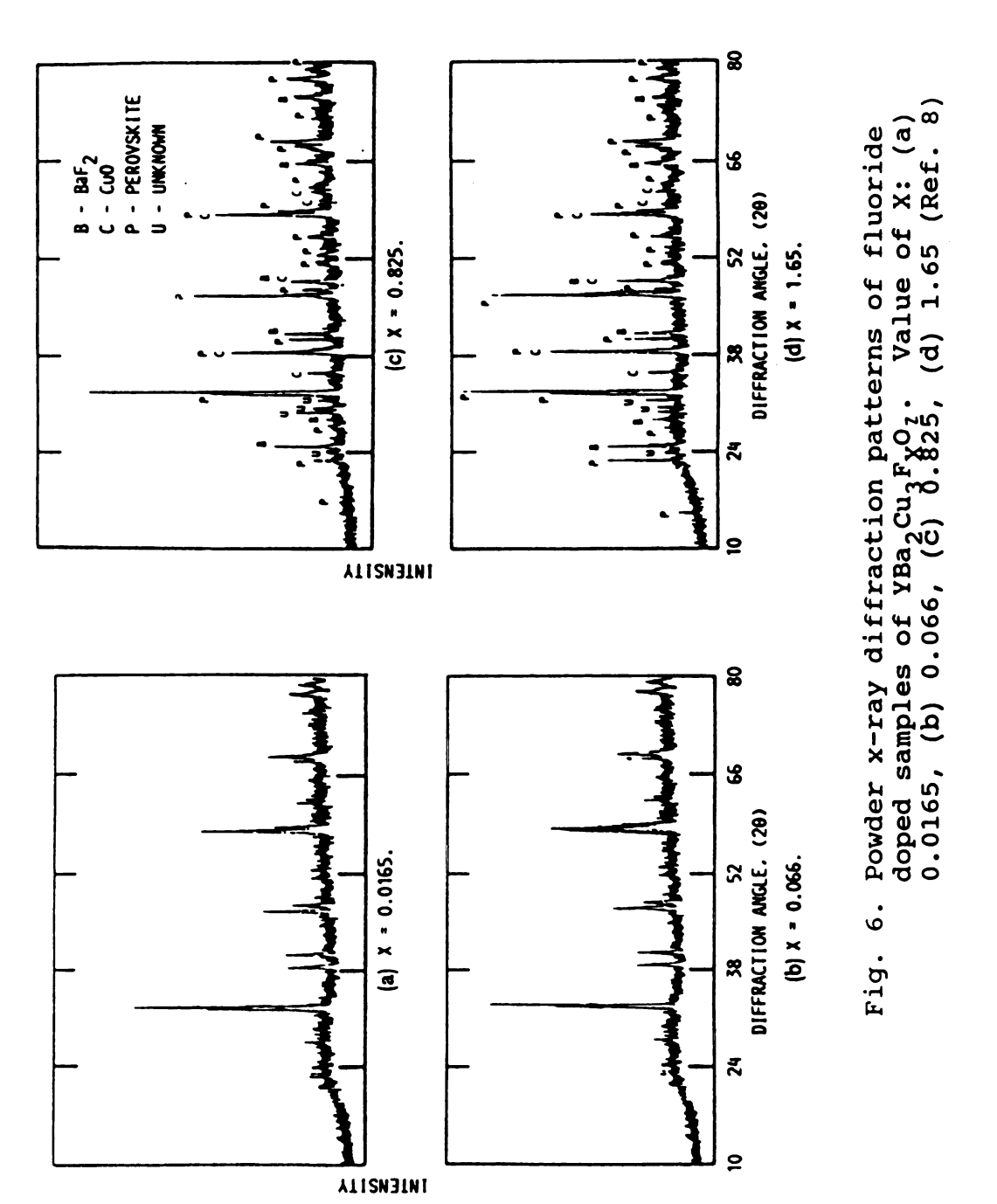


Fig. 5. Resistance vs temperature measurement of nominal composition YBa<sub>2</sub>Cu<sub>3</sub>F<sub>2</sub>O<sub>2</sub>. Curve A shows the resistance upon initial cooling; curve B, data obtained upon second cooling; and curve C, data from warming after second cooling (Ref. 7).

Table 2

Phase Distribution in Samples With Nominal Compositions of YBa $_2$ Cu $_3F_X$ Cl $_Y$ O $_Z$  (Ref. 9)

*	٧	YBa2Cu3O,	Y2BaCuO5	BaF2	BaFCI	CuO	Cu <sub>2</sub> Y <sub>2</sub> O <sub>5</sub>	(BaCu)OCl <sub>2</sub>
								(BaCu)OF <sub>2</sub>
0	0	1.00	0	0	0	0	0	0
_	0	0.33	0.30	0.25	0	0.03	0	0.09
7	0	0.15	0.20	0.48	0	0.05	0	0.12
<b>-</b> 7	0	0	0	0.73	0	0.0	81.0	0
0	_	0.35	0.13	0	0	0	0	0.51
0	7	0.24	0.07	0	0	0	0.14	0.51
0	4	0	0	0	0	0.29	0.50	0
4/3	4/3	0.09	0.26	0	0.45	91.0	0	0.04
_	-	0.26	0.15	0	0.48	0.07	0	0.04



it can be seen that incomplete decomposition of  $BaF_2$  leads to inhomogeneous phase formation as the amount of  $BaF_2$  increases [9]. Since  $BaF_2$  remained intact at the sintering temperature, part of the barium source was unavailable to form the superconducting phase.

Although Narottam et al. [8] find no proof for the very high  $T_c$ 's reported by Ovshinsky et al. [7], their results indicate that superconducting critical temperature is both slightly increased and sharpened with low levels fluorine concentration. Data presented in Table 3 indicates that the value of  $T_c$  increases systematically with concentration of  $T_c$ , reaches a maximum value of 93.4K for  $T_c$  0.066, and then drops with further increase in fluorine concentration. The transition is sharpest for  $T_c$  0.066 and the 10 to 90% transition is within 0.7 t 0.1K of the  $T_c$  for this composition [8].

In Table 4, critical temperatures reported by Yan et al. [9] for F and Cl substituted samples are shown. Most samples showed diamagnetic susceptibility starting at a temperature between 89 and 94K. For the samples of high fluorine concentration, X=4, diamagnetic susceptibility was not observed above 4.2K. It is interesting to note that the samples with a relatively high fluorine concentration (i.e, X=2) still have a critical temperature of 93K, though the superconducting phase is reduced to 15% at that substitution level as shown in Table 2.

Table 3 Critical Temperature and Transition Width of Composition of  $YBa_2Cu_3F_XO_z$  (Ref. 8)

Sample	Value of x	$T_c$ (midpoint) (K)	ΔT <sub>.</sub> (10–90%) (K)
Υ1	0.0165	90.8	0.9
Y2	0.033	92.1	0.8
Y3	0.050	92.5	0.8
Y4	0.066	93.4	0.7
Y5	0.165	92.2	0.8
Y6	0.330	91.6	1.4
Y7	0.825	90.5	3
Y8	1.65	90.3	2.4

Table 4 The Superconductivity Data of Nominal  $YBa_2Cu_3F_XCl_YO_Z$  Compositions (Ref. 9)

x	y	$T_{\rm c}(\chi)^*$	$T_{0}(\varrho)^{*}$	$T(\varrho=0)$
0	0	94	94	92
1	0	94	93.8	91
2	0	93	93.3	<b>89</b> .6
4	0	< 4	· †	
0	l	92	94.3	88.4
0	2	< 4	†	
0	4	< 4	†	
4/3	4/3	89	93.0	< 79
ĺ	1	93	93.8	89.8

#### 3. EXPERIMENTAL PROCEDURE

### 3-1 Sample Preparation

Samples were prepared with three different compositions, i.e., nominal compositions of  $YBa_2Cu_3I_XO_Z$  (where X = 1,2,3 and Z = 5.5, 4.4 and 3.0 respectively ) by mixing stoichiometric quantities of high purity  $Y_2O_3$ ,  $BaCO_3$ , CuO and CuI powders. The powders were weighed on a calibrated metter micro balance.

The powdered mixtures were first mixed in a pestle and mortar, the mixed powder was then placed in an alumina crucible and calcined in oxygen atmosphere at 930°C (1203K) for about 12 hours. The furnace was then turned off and the calcined mixtures were allowed to cool slowly with the furnace door closed. The resulting powder had a dark gray to black appearance like a lump of charcoal at room temperature. The calcined powder was reground and recalcined under similar conditions to achieve a well calcined compound. The chemical reaction for calcination and sintering of the three compounds used in present study are the following:

$${}_{3}^{1}Y_{2}O_{3} + 2BaCO_{3} + 2CuO + CuI = YBa_{2}Cu_{3}I_{1}O_{5.5} + 2CO_{2}$$
 (1)

$$\frac{1}{4}Y_2O_3 + 2BaCO_3 + CuO + 2CuI = YBa_2Cu_3I_2O_{4.5} + 2CO_2$$
 (2)

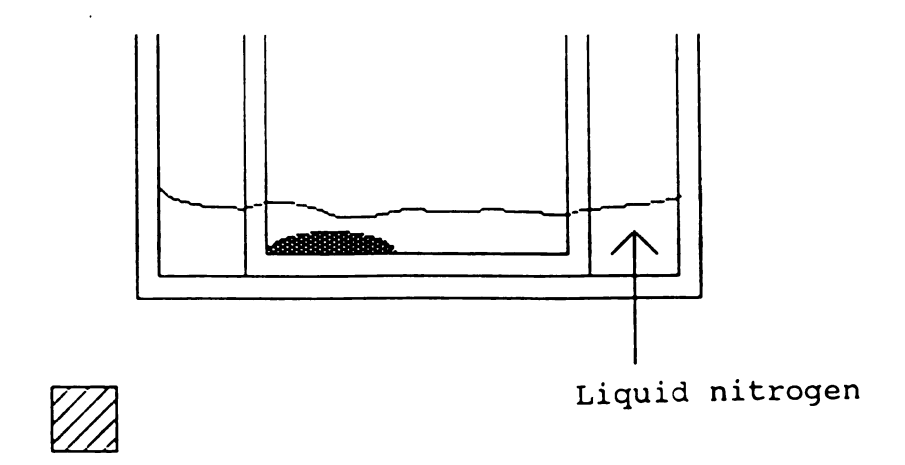
$$\frac{1}{2}Y_2O_3 + 2BaCO_3 + 3CuI = YBa_2Cu_3I_3O_{3.5} + 2CO_2$$
 (3)

# 3-2 Magnetic Separatiton and Sintering

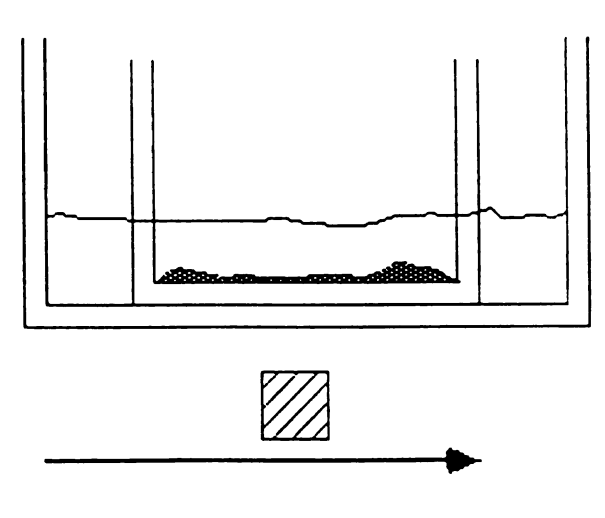
After double calcination, magnetic separation was carried out to enrich the superconducting powders under liquid nitrogen temperature.

The magnetic separation procedure is summarized in Fig. 7, where the double calcined powder was placed at one end of a pyrex beaker. The pyrex beaker was then cooled in liquid nitrogen which was stored at larger pyrex vessel and then a permanent magnet was moved over the pyrex beaker. The superconducting phase, pushed away by the magnetic field, accumulated at one end of pyrex beaker. The non-superconducting phase, unreacted powder, does not respond to the field and remains stand still. During the magnetic separation, very fine particles of calcined powders were not responsive to the field and stuck together with some moisture. Barsoum et al. [24] reported another possible problem related to separation, namely the very fine impurity can be embedded in the relatively large superconducting particles and are carried along with the superconducting powders. To prevent very fine impurity from getting embedded and to obtain further purification, the magnetically separated superconducting particles were grounded and separated again under same conditions, as mentioned above.

As discussed later, the magnetic separation plays a possible role in removing impurity as judged from x-ray dif-



a)



Moving magnet

b)

Fig. 7. Schematic diagram of the magnetic separation procedure. (a) Before doing magnetic separation (b) Under moving magnet

fraction studies.

The magnetically separated powders, mixed with a binder, were cold pressed into one inch diameter pellets at a pressure of 10,000 psi and then sintered at 950°C (1223K) for 12 hours in an oxygen atmosphere. Amyl acetate was used as the binder. The sintered pellets were slowly cooled to room temperature in the furnace by turning the furnace off.

A continuous measurement of temperature dependence of resistance was carried out by means of a LR-400, four wire AC resistance bridge and a Houston instrument 200, X-Y recorder. Liquid nitrogen placed in a deep, wide mouth dwer flask was used for cooling the sample.

Fig. 8 shows a schematic of the 4 wire AC resistance measurement compound. Four gold plated wire pins were attached to the sample. The two outer ones were used for current supply and the inner two were used for voltage measurement.

Four standard gold plated wire wraped socket pins, laid against one face of the sample, as shown in Fig. 9, were used to make contact for measuring the AC resistance of the superconducting sample. A copper-constantan thermocouple was attached to the center of specimen. The sample and pins were wrapped between two polyvinylchloride (PVC) blocks. All were then clamped together with two small plastic clamps, as shown in Fig. 10. The entire assembly was immersed very slowly in the liquid nitrogen flask.

Temperature was monitored by a digital thermometer. The uncertainity in the temperature measurement was estimated to be approximately  $\pm$  0.5K.

The electrical resistance was monitored by using the LR-400 AC resistance bridge in the temperature range from room temperature to liquid nitrogen temperature (77K). The

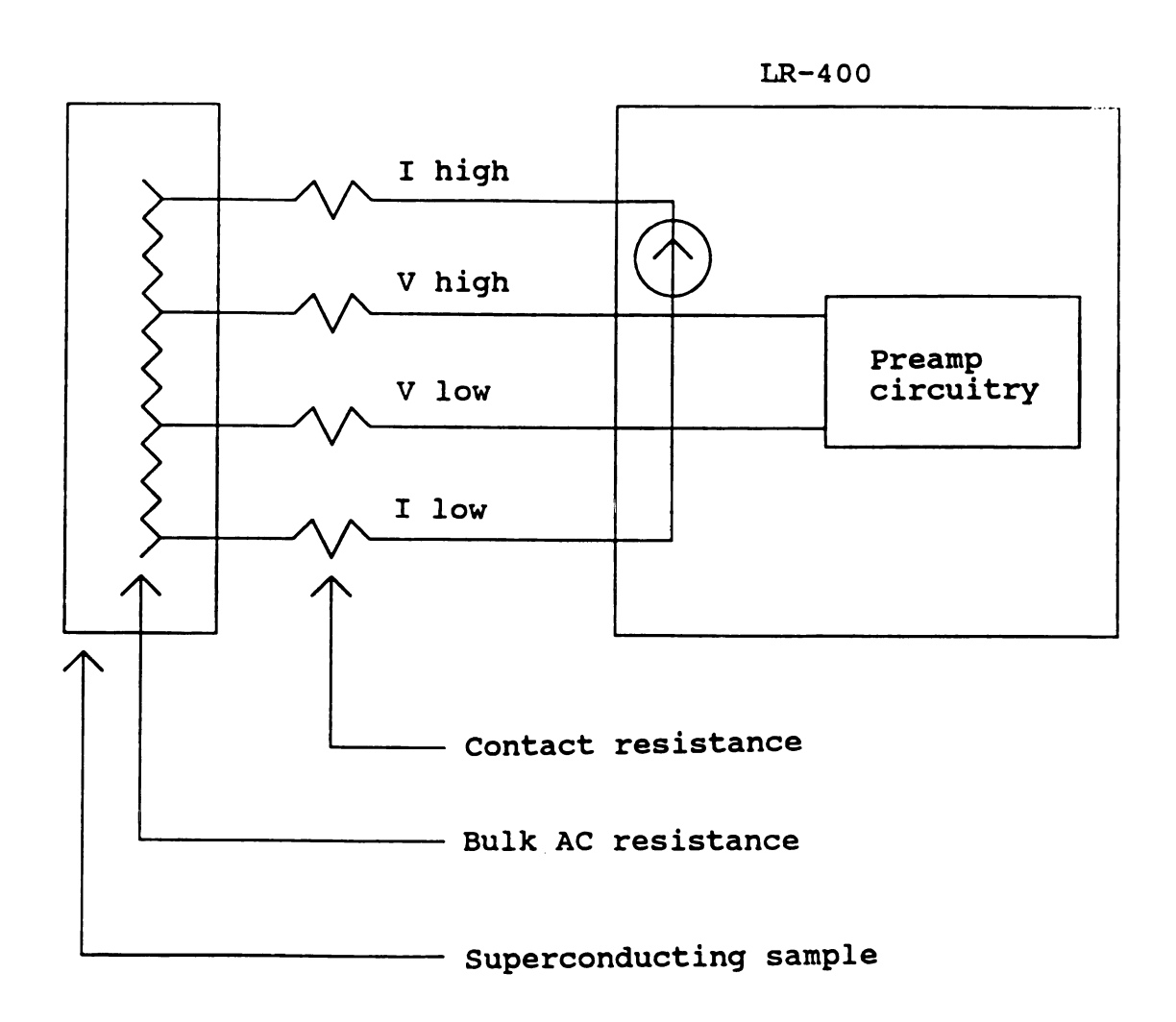


Fig. 8. Schematic of 4 wire AC resistance measurement

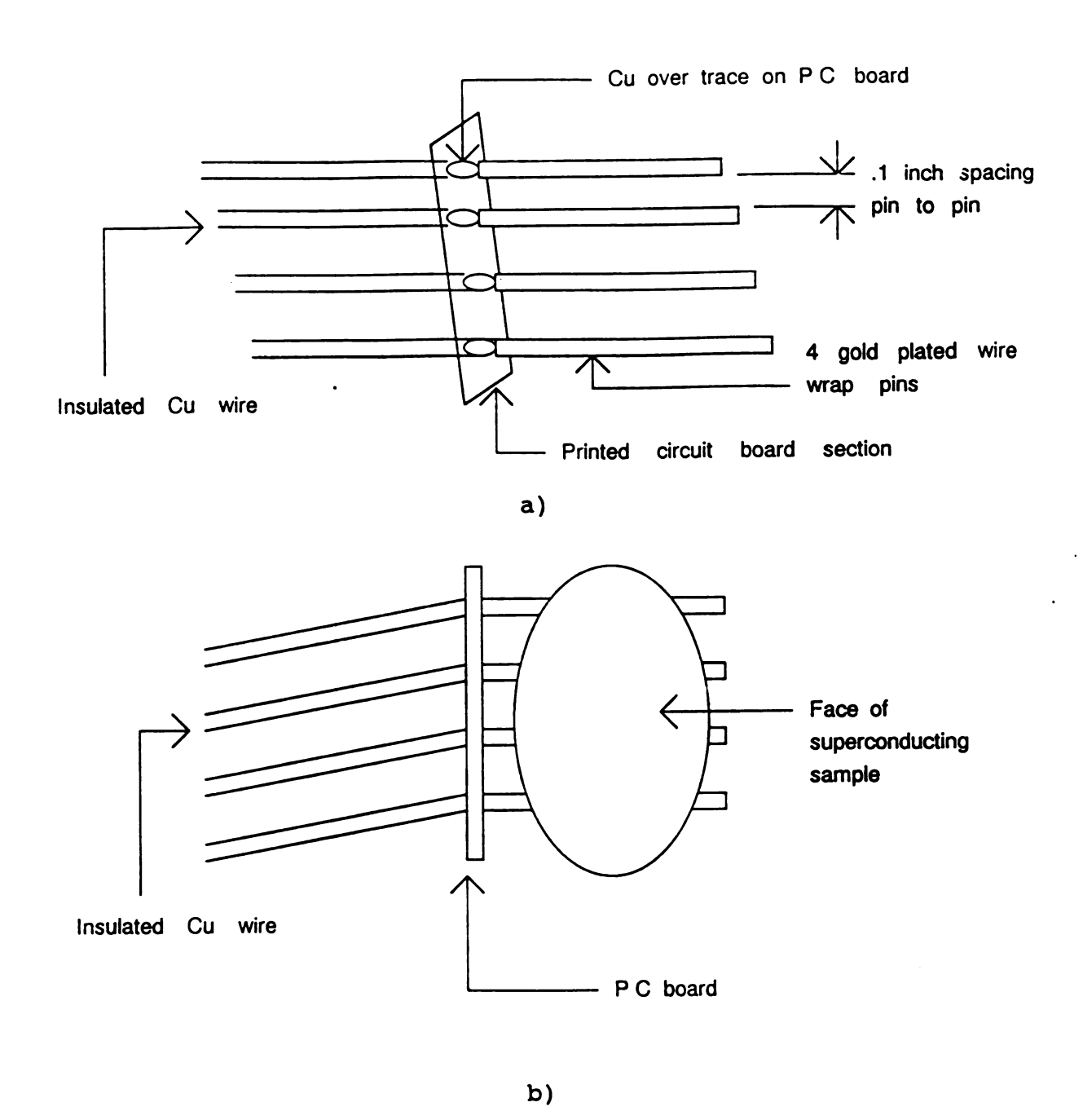


Fig. 9. Schematic of (a) 4 gold plated wire (b) with superconducting sample

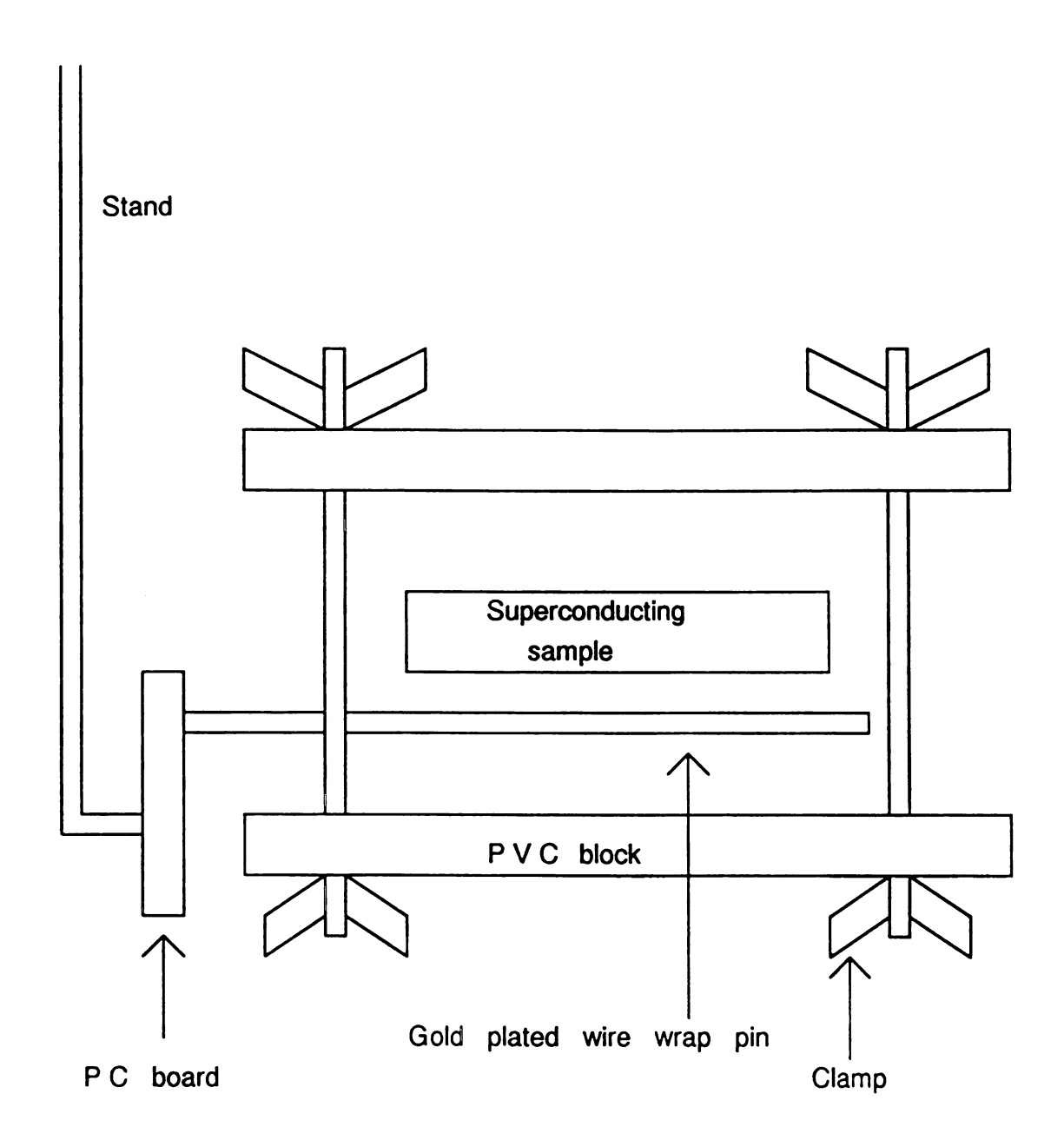


Fig. 10. Sample holder assembly for 4 contact direct AC resistance measurement

resolution of that machine is 1 micro ohm. The excitation current used for this study was 3 mili ampere. Fig. 11 shows the schematic diagram of electrical resistance measurement set-up.

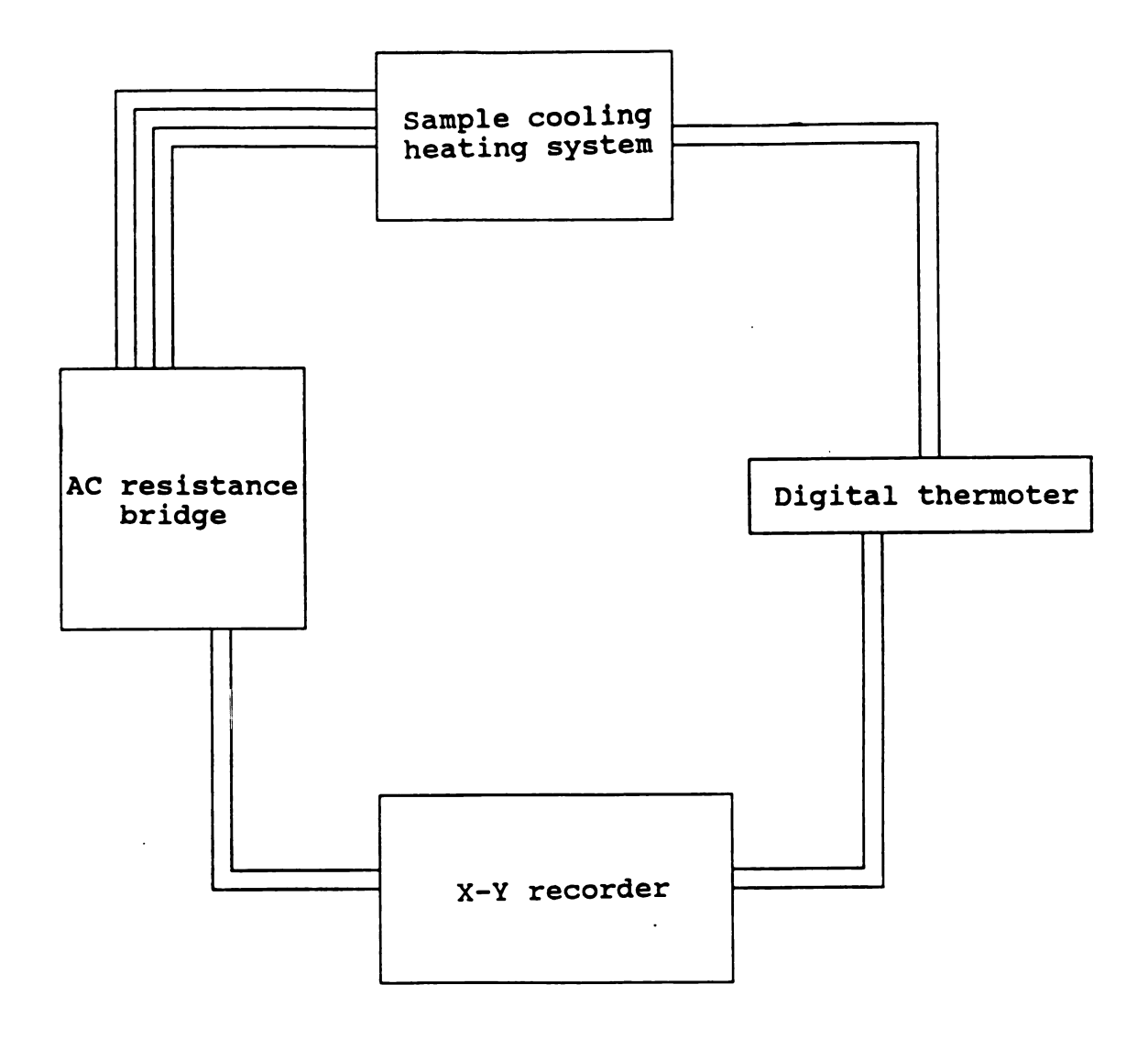


Fig. 11. Schematic diagram of resistance measurement set-up.

The YBa<sub>2</sub>Cu<sub>3</sub>IO<sub>5.5</sub> samples were cut into rectangular bars with cross sectional area of 0.01Cm<sup>2</sup> by using a diamond blade. The contacts sulfaces of the cut samples were painted with silver. After drying for one hour, leads were attached to the silver contacts by using the same silver paint.

Upon measuring critical current density, it was observed that the contacts were partially melted due to high contact resistance resulting from poor contact. Thus, a set of new samples were prepared under same condition except for the contact method. Silver paint contacts were painted on the top surface of sample and then the samples were annealed at 950°C for 3 hours in the furnace in order to reduce the contact resistance. Recent studies indicate that the silver could fill the pores of surface contact and lower the intergrain resistances during high temperature sintering [25,26].

After 3 hours of heat treatment, the samples were slowly cooled to room temperature in the furnace. Leads were attached to the heat treated silver contacts by using the same silver paint, as discussed.

The critical current density,  $J_c$  , measurement was performed by using a conventional two probe technique.  $J_c$  is determined by the sudden voltage rise due to the increase of resistance associated with the superconducting to normal state transition at the current density equal to  $J_c$ . Fig. 12

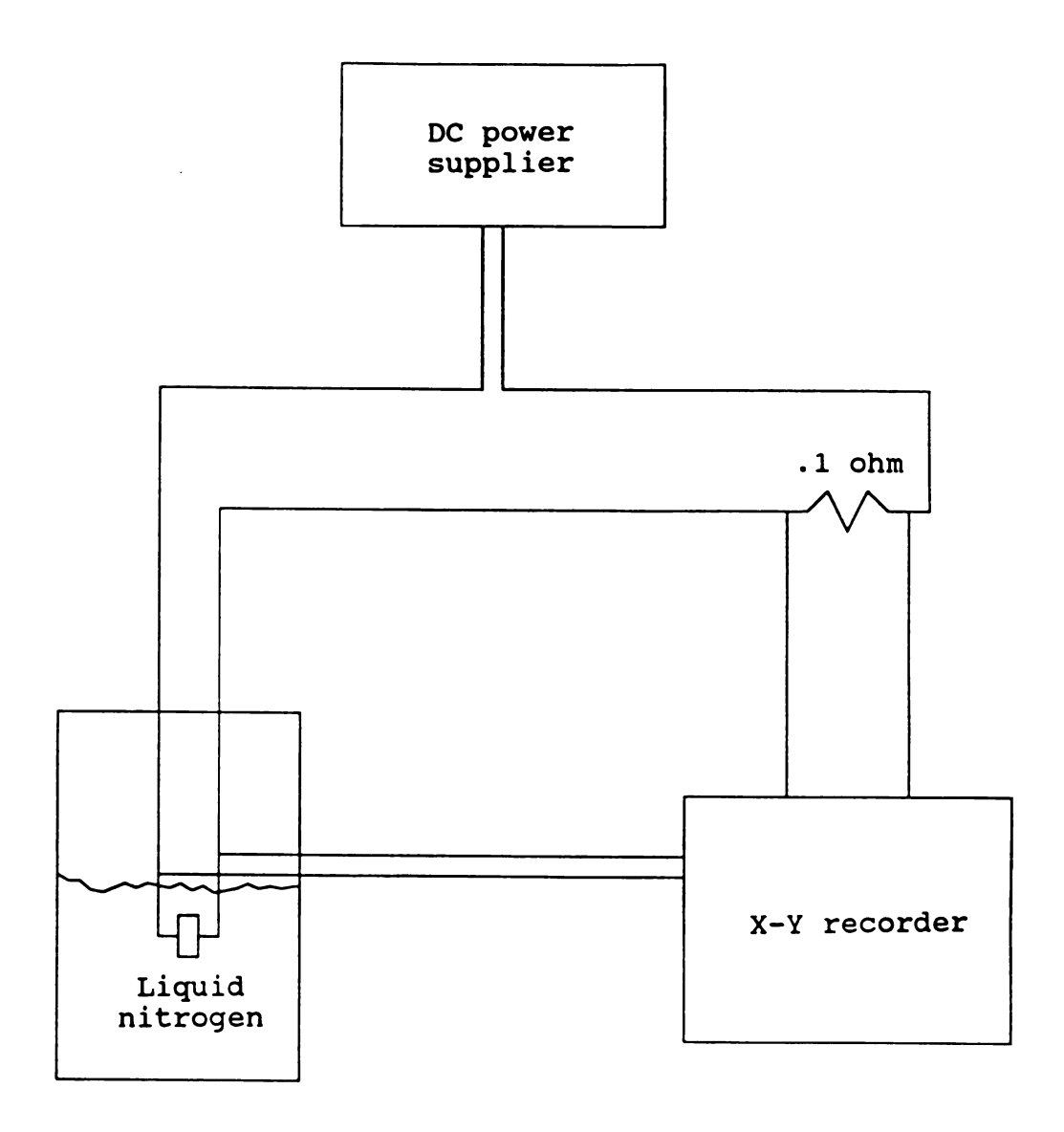


Fig. 12. Schematic diagram of  $J_{c}$  measurement set-up

shows a schematic diagram of the critical current density measurement set-up.

The critical current density values were measured at liquid nitrogen temperature (77K). The applied current range was from 0.1 to 6 ampere and the critical current density was calculated to be  $Amp/Cm^2$ .

# 3-5 EDAX and X-Ray Measurement

To confirm the presence of iodine in samples, EDAX analysis was carried out. A Tracor 5500 EDAX system was used for this purpose.

X-ray diffraction experiments were conducted by using  $\text{Cu K}\alpha$  radiation. Sintered pellet samples were used for this purpose.

## 3-6 Morphological Examination

## 3-6-1 Scanning Electron Microscopy

Transverse fractured sections of specimens were mounted on cylindrical aluminium stubs. To avoid surface charge, the mounted sample surfaces were coated with pure gold by argon sputtering of gold target at a pressure of 0.1 torr. Silver paint was used for electrical contact to ground and also to provide a better mechanical support.

A Hitachi 415C scanning electron microscope was used for microstructural investigations.

## 3-6-2 Optical Microscopy

The samples were metallographically mounted on Lucite blocks and initially ground on 600 grade emery paper. For further polishing, a 5 micron alumina powder, dispersed in methanol (in stead of distilled water) was used to prevent any possible degredation of the superconductor due to moisture up take. The samples were polished on a nylon cloth, using diamond paste of the size from 2 micro to 0.5 micrometer. Photo micrographs were taken at magnifications as high as 2000X.

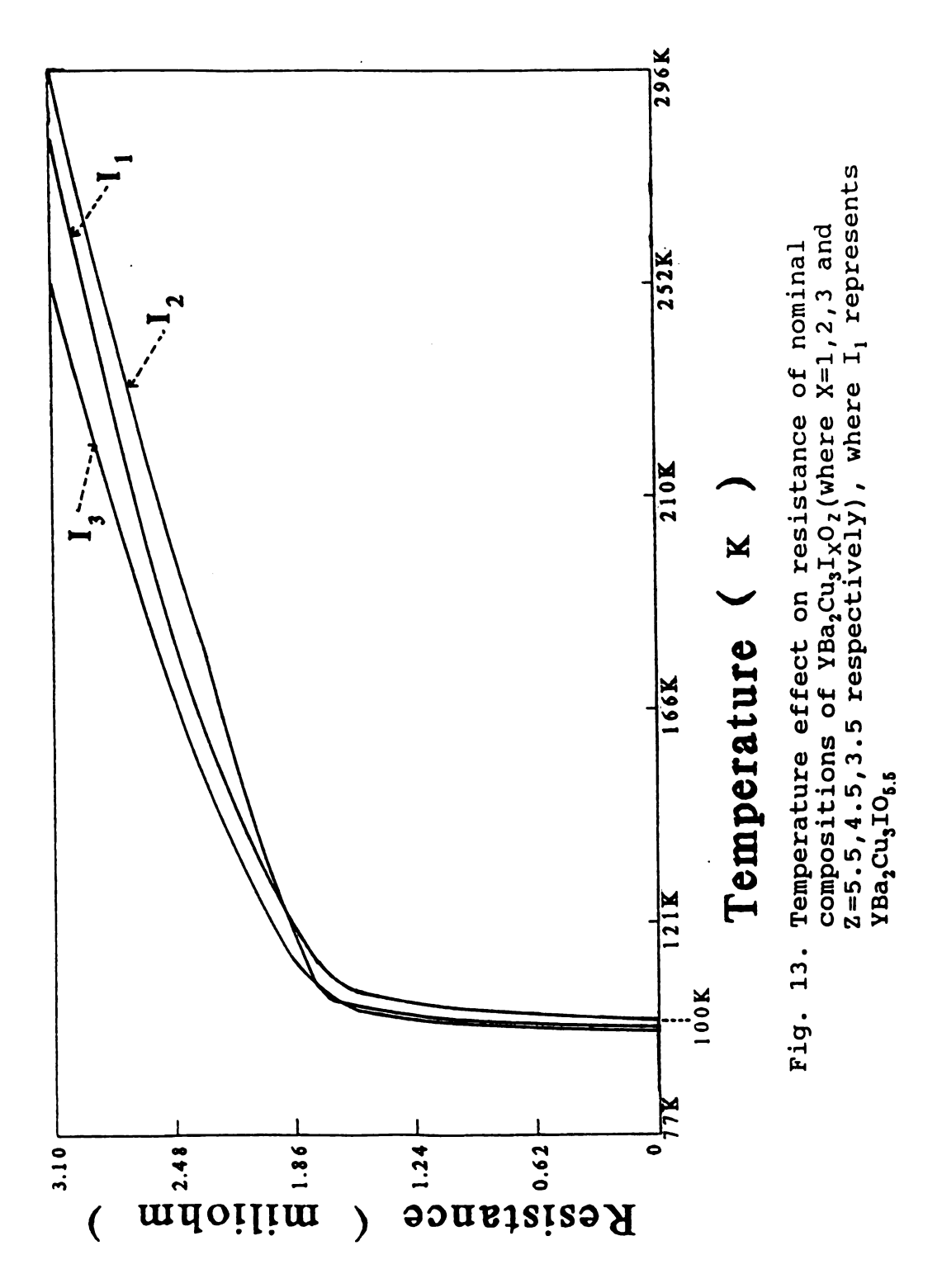
#### 4. RESULTS AND DISCUSSION

### 4-1 Critical Temperature Measurement

The temperature effect on electrical resistance for samples with iodine stoichiometry of 1,2 and 3 are shown in Fig. 13. It is observed that the resistance of composition with 1 iodine showed zero resistance state at a temperature of 100K and onset of rapid loss of resistance occured at 110K.

The samples with iodine stoichiometries of 2 and 3 possess a slightly higher critical temperature than that for the conventional 1:2:3 materials:(97K for iodine 2 sample, 96K for iodine 3 sample). The maximum critical temperature of conventional 1:2:3 samples was reported to be in the range of 90 to 95K [1,27]. Our own measurements of T<sub>c</sub> (using our measuring system) also indicate a T<sub>c</sub> of 93 to 95K. The overall shape of the curve is similar to a metallic to "semiconductor-like" transition which is often found when a 3-d transition metal is substituted in Y-Ba-Cu-O compound.

It should be noted that a high substitution level of iodine (eg. iodine 3) does not degrade the superconductivity, unlike F and Cl substitutions. To the contrary, it was observed that even at a level of iodine 3, the critical temperature is slightly higher than that for no iodine substitution.



In order to determine reproducibility of results, resistance measurements conducted with consecutive cooling and heating cycles. Result from one such measurements for composition of iodine stoichiometry of 1 is shown in Fig. 14. Upon cooling, the resistance starts to decrese gradually and then decrease abruptly at 110K. The sample with one iodine looses almost 60% of its resistance at this onset temperature and finally zero resistance state is reached at 100K. Upon heating, the sample remains in the zero resistance state up to about 102K and then the resistance begins to increase very sharply and the normal state is reached at 110K. After coming back to room temperature, a very small hysteresis of resistance was observed.

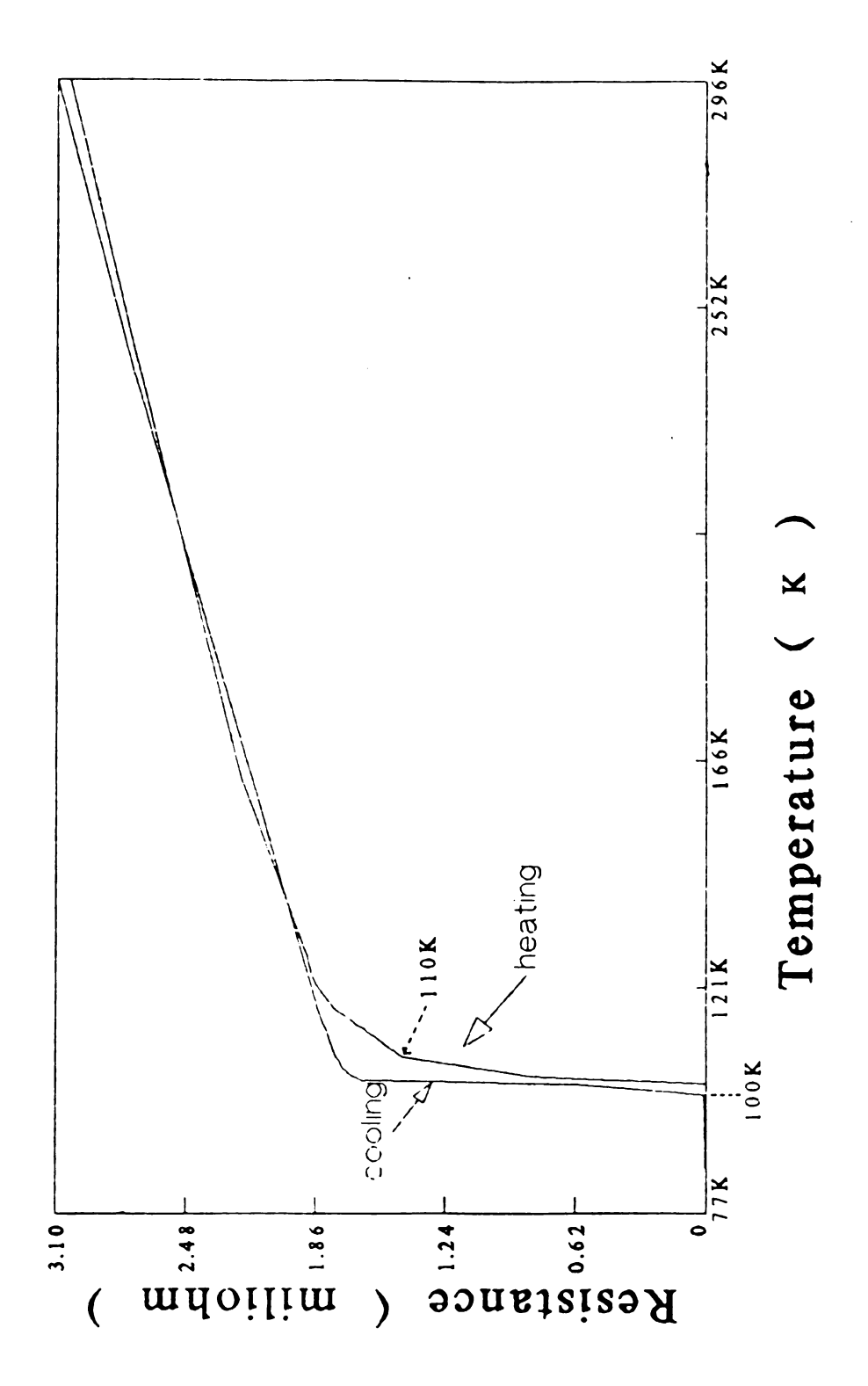


Fig. 14. The cooling and heating cyclic measurement of the resistance of  $YBa_2Cu_3IO_{5.5}$ 

### 4-2 Critical Current Density Measurement

The critical current density measurements were performed at liquid nitrogen temperature (77K). The current-voltage curve of sample YBa<sub>2</sub>Cu<sub>3</sub>IO<sub>5.5</sub>, which is rectangular bar with cross sectinal area of 0.01Cm<sup>2</sup>, is shown in Fig. 15. It can be seen that the overall shape of current-voltage curve is similar to that of a conventional 1:2:3 compound except for the increase in voltage due to contact resistance. Ideally, the base line should be nearly parallel to the x-axis.

As the applied current increases, first the voltage increases gradually and then rises abruptly at the limiting value of current, which is defined is the critical current for this sample. Measured value of critical current density is found to be around  $320 \text{ Amp/cm}^2$ . This value is slightly higher than that for the bulk  $YBa_2Cu_3O_{7-X}$  samples without any special sample preparation techniques, i.e., field oriented grain method, or texture formation etc. [25,28]. As stated earlier, samples with silver contacts, which are not heat treated and thus have high contact resistance, show either partially melted or broken contact. These high contact resistance samples initially show an abrupt rise in voltage on a current-voltage (I-V) curve. Thus for the best value of  $J_c$ , the contact resistance must be reduced as much as possible.

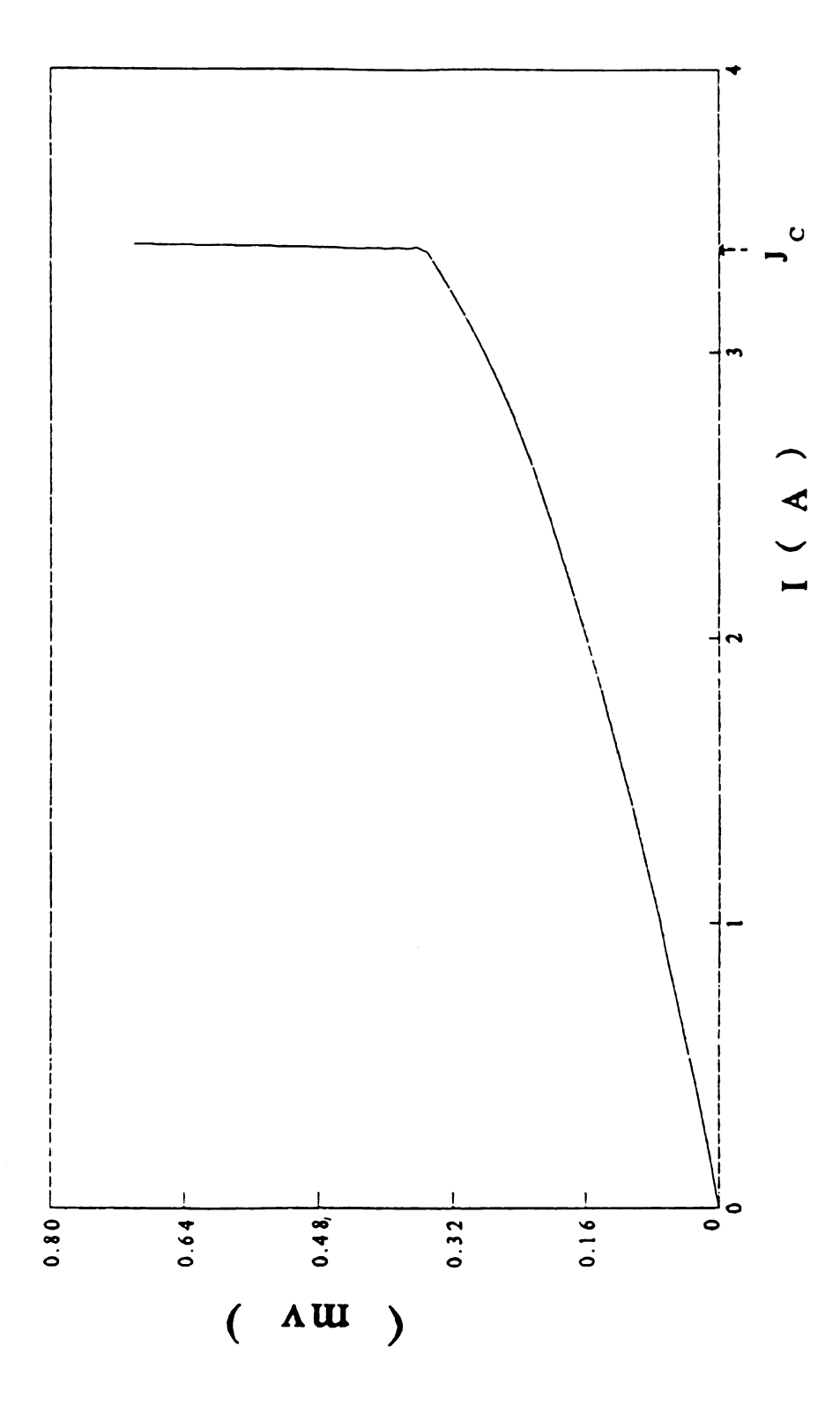


Fig. 15. Current-voltage curve of YBa<sub>2</sub>Cu<sub>3</sub>IO<sub>5.5</sub>

The heat treated silver contact samples give us the most reasonable critical current value, even though these samples still have a small contact resistance(0.08 miliohm). The best measured I-V characteristics are shown in Fig. 15.

Chen et al. [25] reported that the silver essentially fills the surface pores of granular YBa<sub>2</sub>Cu<sub>3</sub>O<sub>7-X</sub> samples as judged from their microscopic studies. This pore filling improves the contact between grains and hence reduces the contact resistance.

It is interesting to note that the measured value of  $J_c$  for iodine 1 samples is 320 Amp/cm<sup>2</sup> and this value is comparable to that for silver oxide substituted 1:2:3 compound repoted by Peters et al. [26].

### 4.3 EDAX And X-Ray Measurements

Fig. 16 shows the result of energy dispersive X-ray analysis for the YBa<sub>2</sub>Cu<sub>3</sub>IO<sub>5.5</sub> sample, and fig. 17 and 18 show the EDAX spectra from I2 and I3 compositions respectively. Data label represent the intensity of elements in terms of counts. These results are qualitative only since no corrections (such as absorption correction etc.) were made. It was, however, observed that the number of counts of iodine systematically increased, in the ratio of 362: 563: 709 which is approximately 1: 1.5: 2 as the concentration of iodine increased. It is not known why the small peak of sulfur (which is around 2.3keV in Fig. 17-18) was detected for I2 and I3 compositions while that peak was not detected for I<sub>1</sub> sample. Sulfur, however, is known for improve superconducting properties of 1:2:3 compound such as the critical field, and the sharpness of transition temperature range [29].

Fig. 19.(a) shows the x-ray diffraction patterns of 1:2:3 compound and 19.(b) shows that for the  $I_1$  sample. Comparing x-ray diffraction patterns for 1:2:3 compound and the  $I_1$  sample, it is observed that all the peaks are similar except that the low angle back ground intensity of the magnetically separated iodine 1 sample is noticeable less. It can be considered that the magnetic separation helps to

TN-5500

Cursor: 0.000KeV = 0 R0I (4) 0.000: 0.000

END CURSON: 0.0000

END CURSON: 0.000

MEM (11), 0.010keV LT= 120SECS LABEL:EXEC(7-C) DATA LABELI-1

EXEC(7-0) DATA LABELI-1

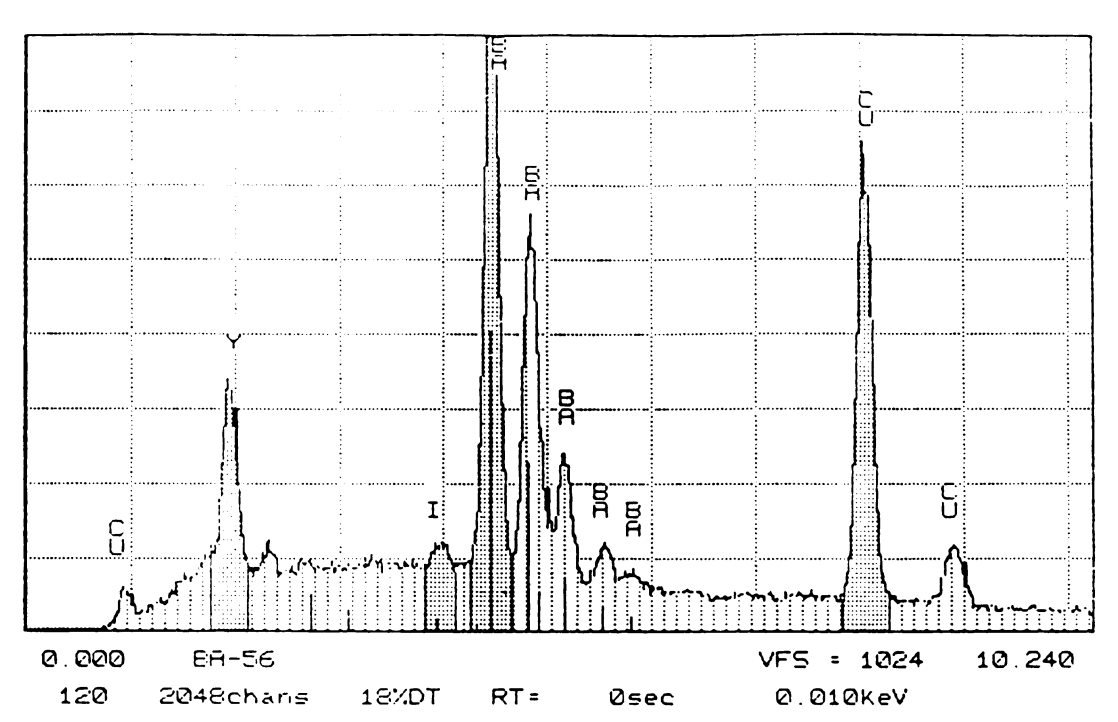
120

Y	Ó (	00]	1.770: 2.120keV	GROSS=	10541	NET=	5466
I	1 C	Ø1]	3.820: 4.110keV	GROSS=	4335	NET=	362
Ва	2 C	Ø2]	4.270: 4.650keV	GROSS=	23397	NET=	18096
Cu	3 [	031	7.830: 8.280keV	GROSS=	15858	NET=	12843

Fig. 16. The EDAX spectra of  $YBa_2Cu_3IO_{5.5}$  sample

TN-5500

Curson: 0.000keV = 0 R0I (4) 0.000: 0.000



MEM (11), 0.010keV LT= 120SECS LABEL:EXEC(7-C) DATA LABELI-2

Y	Ø [	ØØ]	1.770:	2.120keV	GROSS=	9071	NET=	4241
I	1 C	<b>01</b> ]	3.820:	4.110keV	GROSS=	3884	NET=	563
Ва	2 C	02]	4.270:	4.650keV	GROSS=	21992	NET=	17204
Cu	3 L	കമാ	7 830·	8 280keV	GEOSS=	16184	NET=	13169

Fig. 17. The EDAX spectra of  $YBA_2Cu_3I_2O_{4.5}$  sample

MEM (11), 0.010keV LT= 120SECS LABEL:EXEC(7-C) DATA LABELI-3

EXEC(7-0) DATA LABELI-3

120

Y 0 [ 00] 1.770: 2.120keV GROSS= 7147 NET= 3822 I 1 [ 01] 3.820: 4.110keV GROSS= 3232 NET= 709 Ba 2 [ 02] 4.270: 4.650keV GROSS= 18777 NET= 14274 Cu 3 [ 03] 7.830: 8.280keV GROSS= 13274 NET= 10934

Fig. 18. The EDAX spectra of  $YBa_2Cu_3I_3O_{3.5}$  sample

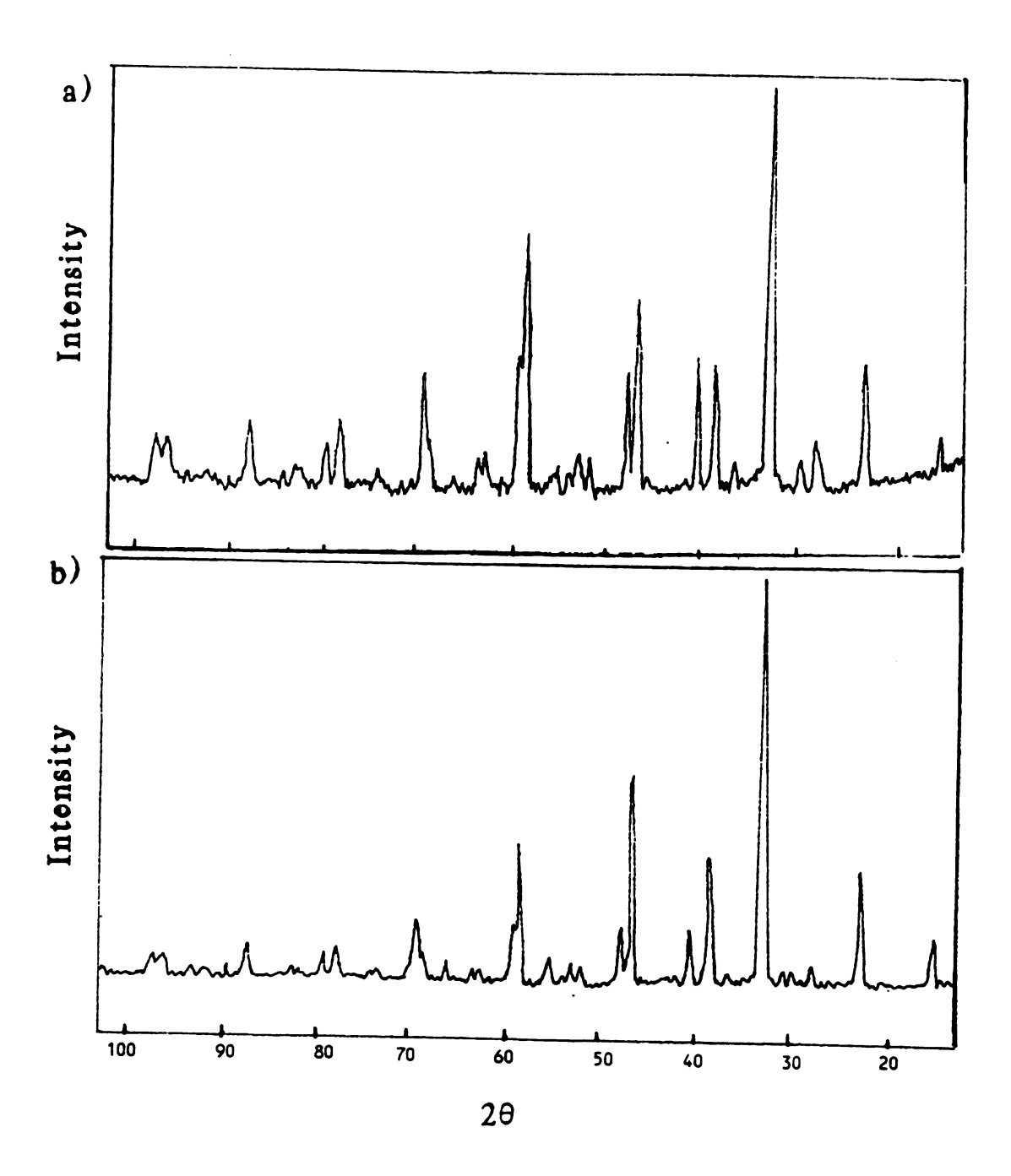


Fig. 19. X-ray diffraction patterns of a) 1:2:3 sample b) YBa<sub>2</sub>Cu<sub>3</sub>IO<sub>5.5</sub> sample

remove noncrystalline(glassy) or microcrystalline particles, which is unseparated samples contribute to the low angle back ground intensity. Fig. 20 and 21 show the x-ray diffraction patterns of  $I_2$  and  $I_3$  samples. Once again magnetically separated samples show lower back ground intensity at lower angles.

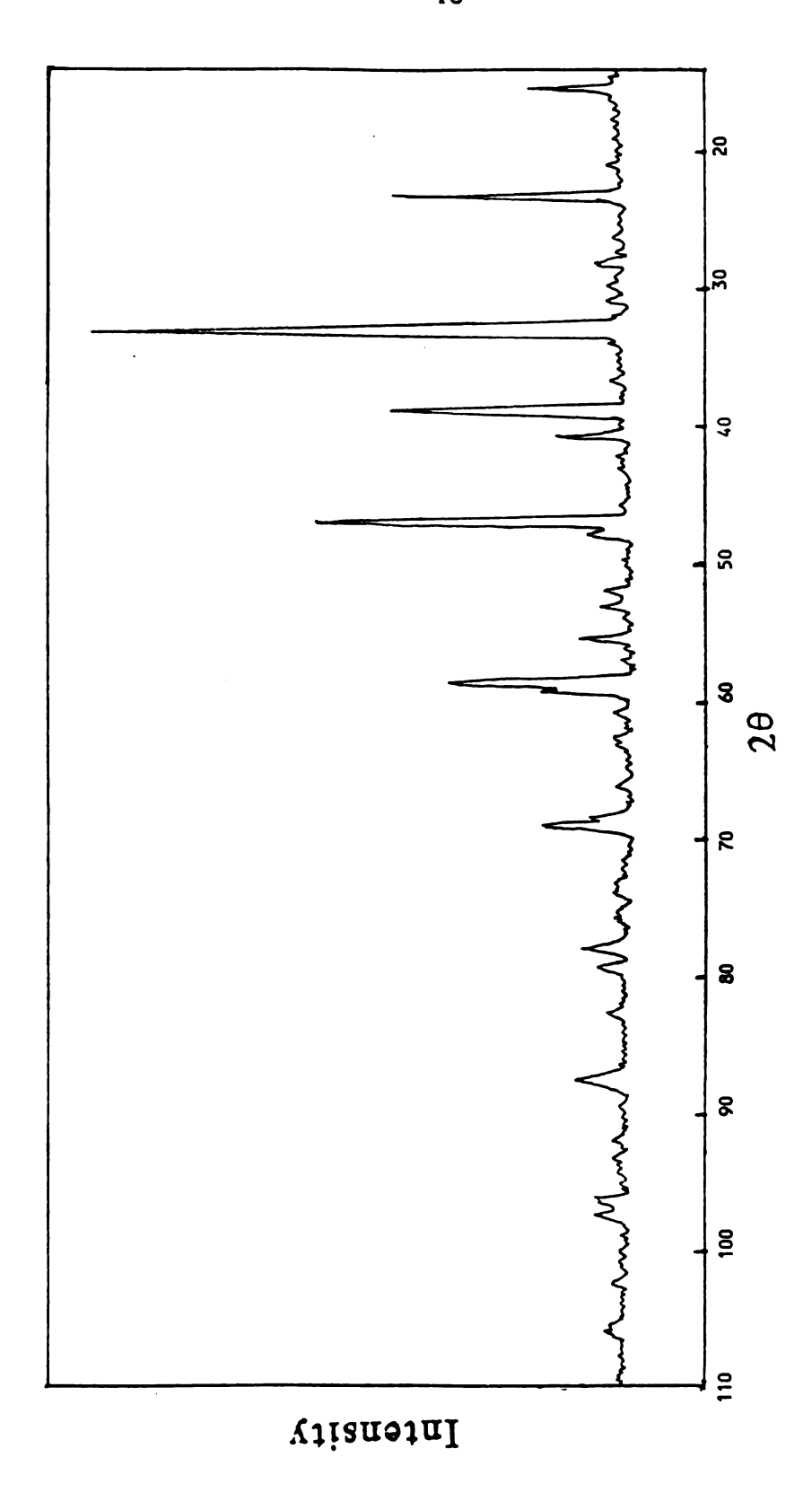


Fig. 20. X-ray diffraction patterns of  ${\rm YBa_2Cu_3I_2O_{4.5}}$  sample

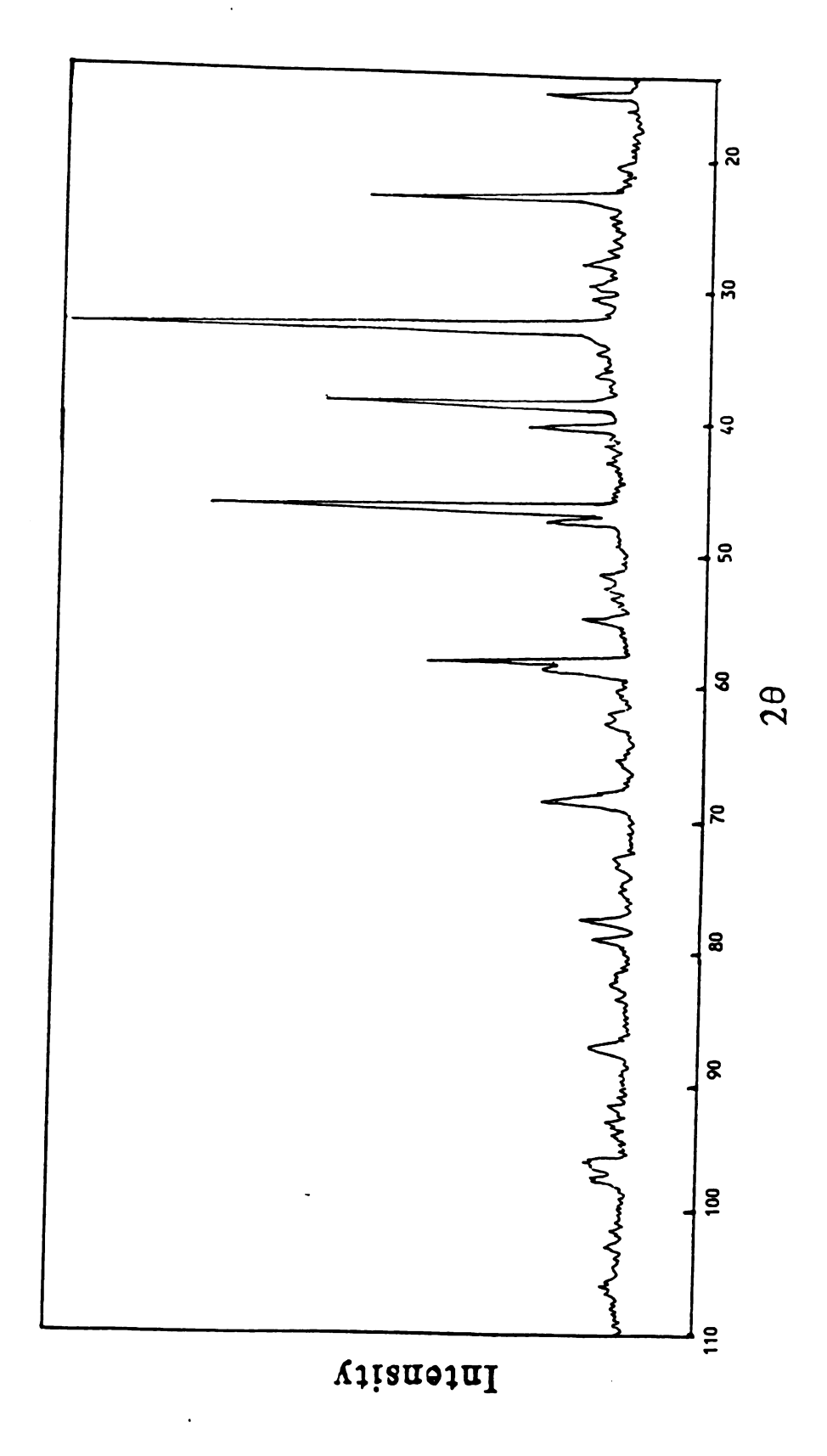


Fig. 21. X-ray diffraction patterns of YBa2Cu3I3O3.5 sample

### 4-4 Microstructures of Iodine Substituted 1:2:3 sample

The optical micrographs and SEM micrographs of YBa<sub>2</sub>Cu<sub>3</sub>-I<sub>X</sub>O<sub>Y</sub> (X=1,2,3 and Y=5.5,4.5,3.5 respectively) are shown in Fig. 22-25. The microstructure of iodine substituted 1:2:3 samples show well formed twinning within the grains resulting from tetragonal to orthorhombic transformation. It has been suggested that the role of these twins is to provide strain accomodation during transformation which is of the martensitic type [30]. Optical micrographs show relatively thick and irregular twins in some grains as shown in Fig. 22. Comparative transformation twins in 1:2:3 samples are much finer.

A correlation between these twins and superconducting properties, such as  $T_c$  and  $J_c$ , has been suggested by many authors but the subject is controversial [20,31]. Deutscher et al. [20] claimed that twin boundaries play a role in blocking supercurrent, supported by single crystal current density measurements [17] and other magnetization measurements of powdered 1:2:3 materials [32]. They explained that for currents flowing in the Cu-O plane, currents do not have to cross (001) twin boundaries while currents must cross both (001) and (110) twin boundaries for currents flowing perpendicular to the Cu-O plane. However, Chauhari et al. claimed that twin boundaries act as strong pinning sites for the flux lines [31], and thus improve  $J_c$ .

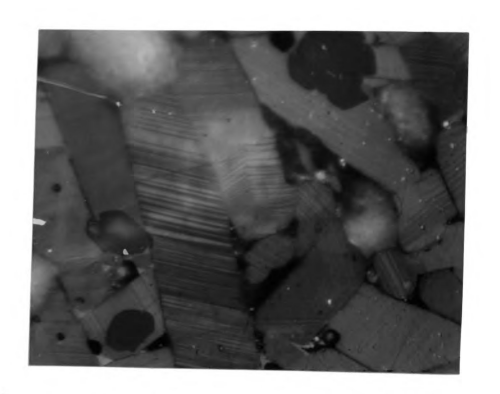
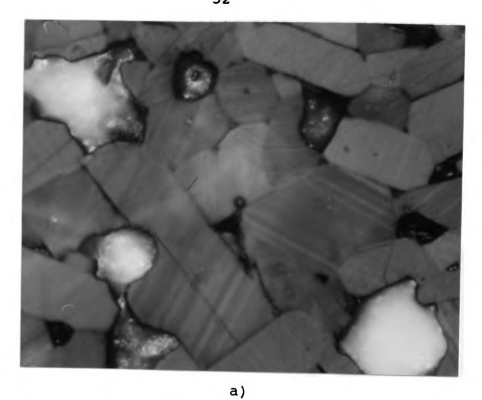


Fig. 22. Optical microscopy of YBa<sub>2</sub>Cu<sub>3</sub>IO<sub>5.5</sub>



b)

Fig. 23. Optical microscopy of a)  $YBa_2Cu_3I_2O_{4.5}$  b)  $YBa_2Cu_3I_3O_{3.5}$ 

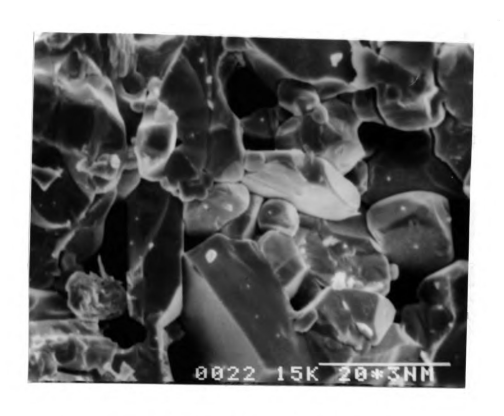


Fig. 24. SEM micrograph of YBa<sub>2</sub>Cu<sub>3</sub>IO<sub>5.5</sub>

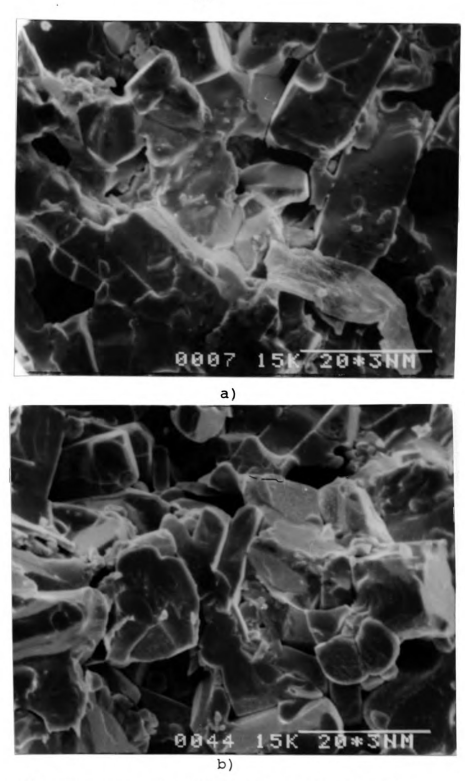


Fig. 25. SEM micrograph of a)  $YBa_2Cu_3I_2O_{4.5}$  b)  $YBa_2Cu_3I_3O_{3.5}$ 

It can be speculated from our results being a help in reducing barrier to supercurrent flow. Although that theory can not explain weak Josephson junction between grain boundaries, it might explain the existence of a small fraction of particles (internal boundary free) with have higher than average  $T_{\rm c}$ .

#### 5. SUMMARY

In the present study the superconducting properties of iodine substituted Y-Ba-Cu-O compounds were investigated using CuI as the agent for iodine substitution. The critical temperature and critical current density measurements, the EDAX and x-ray analysis and the SEM and optical microscopy examinations were employed to study the electrical properties, to determine the iodine stoichiometry and to examine the microstructures of these compounds respectively. Following are the main conclusions of this study:

- 1. EDAX analysis show that the relative intensity of iodine in the lattice increases as the nominal concentration of iodine increases in these compounds.
- 2. Unlike Fluorine and Chlorine substituted Y-Ba-Cu-O compounds, the high substitution levels of iodine, eg., YBa<sub>2</sub>Cu<sub>3</sub>I<sub>3</sub>O<sub>3.5</sub> do not destroy superconductivity.
- 3. A relatively higher critical temperature ( critical temperature = 100K, onset temperature = 110K) is observed for iodine substituted YBa<sub>2</sub>Cu<sub>3</sub>IO<sub>5.5</sub> superconducting compound.
- 4. Microstructures of these compound show presence of thick and regulary spaced twinned structure which is indicative of the orthorhombic superconducting phase.

#### 6. REFERENCES

- 1. M.K. Wu, J.R. Ashborm and C.W. Chu, Phys. Rev. Lett., 58, 908 (1987)
- 2. H. Hor, R.L. Meng, Y.Q. Wang, L. Gao, Z.J. Huang, J. Bechtold, K. Forster and C.W. Chu, Phys. Rev. Lett., 58, 1891 (1987)
- 3. D.W. Murphy, S. Sunshine, R.B. Dover, R.J. Cava, B. Batlogg and L.F. Scheemeyer, Phys. Rev. Lett., 58, 1888 (1987)
- 4. J.M. Tarascon, L.H. Greene, P. Barboux and G.W. Hull, Phys. Rev., B 36, 8393 (1987)
- 5. Gang Xiao, F.H. Streitz, A. Gavrin and C.L. chien, Phys. Rev., B 35, 8782 (1987)
- 6. M.F. Yan, W.W. Rhodes and P.K. Gallagher, J. Appl. Phys., 63, 821 (1988)
- 7. S.R. Ovshinsky, R.T. Young, D.D. Allred, G. DeMagio and G.A. Van der Leeden, Phys. Rev. Lett., 58, 2579 (1987)
- 8. Narottam P. Bansal and Ann L. Sandkuhl, Appl. Phys. Lett., 52, 838 (1988)
- 9. M.F. Yan, G. Sageev Grader and W.W. Rhodes, J. Mat. Sci., 24, 703 (1989)
- 10. R.M. Hazen, L.W. Finger, R.J. Angel, C.T. Prewitt, N.L. Ross, H.K. Mao and C.G. Hadidiacos, Phys. Rev., B 35, 7238 (1987)
- 11. S.B. Qadri, L.E. Toth, M. Osofsky and S.A. Wolf, Phys. Rev., B 35, 7235 (1987)
- 12. J.E. Greedan and C.V. Stager, Phys. Rev., B 35, 8770 (1987)
- 13. W.I.F. David, W.T.A. harrison and J.D. Grace, Nature 327, 310 (1987)
- 14. F. Beech, S. Miraglia, A. Santoro and R.S. Roth, Phys. Rev., B 35, 8778 (1987)
- 15. F. Galasso, J. Met. June, 8 (1987)
- 16. H. Ledbetter, J. Met. January, 24 (1988)

- 17. T.R. Dinger, T.K. Worthington, W.J. Gallagher and R.L. Sandstrom, Phys. Rev. Lett., 58, 2687 (1987)
- 18. T.K. Worthington, W.J. Gallagher and T.R. Dinger, Phys. Rev. Lett., 59, 1160 (1987)
- 19. T.P. Orlando, K.A. Delin, S. Foner and J.M. Tarascon, Phys. Rev., B 35, 7249 (1987)
- 20. G. Deutscher and K.A. Muller, Phys. Rev. Lett., 59, 1745 (1987)
- 21. P. Chaudhari, R.H. Koch, R.B. Laibowitz, T. Mcguire and R. Gambino, Phys. Rev. Lett., 58, 2864 (1987)
- 22. J.T. Chen, L.E. Wegner and E.M. Logothetis, Phys. Rev. Lett., 58, 1972 (1987)
- 23. J. Narayan, V.N. Shulka, S.J. Lukasiewicz, N. Biunno, R. Singh and S.J. Pennycook, Appl. Phys. Lett., 51, 940 (1987)
- 24. M. Barsoum and D. Patten, Appl. Phys. Lett., 51, 1954 (1987)
- 25. K. Chen, B. Maheswaran, Y.P. Liu, B.C. Giessen, C. Chan and R.S. Markiewicz, Appl. Phys. Lett., 55, 289 (1989)
- 26. P.N. Peters, R.C. Sisk and E.W. Urban, Appl. Phys. Lett., 52, 2066 (1988)
- 27. K. Togano, H. Kumakula, K. Fukutomi and K. Tachikawa, Appl. Phys. Lett., 51, 136 (1987)
- 28. M.K. Malik, V.D. Nair, A.R. Biswas and R.V. Raghavan, Appl. Phys. Lett., 52, 1525 (1988)
- 29. I. Felner and Y. Yeshurun, Phys. Rev., B 36, 3923 (1987)
- 30. C.S. Pande, A.K. Singh and A. DasGupta, J. Met. January, 10 (1988)
- 31. P. Chaudhari, Jpn. J. Appl. Phys., 26, 2023 (1987)
- 32. M. Daeumling, J. Seuntjens and D.C. Larbalestier, Appl. Phys. Lett., 52, 590 (1988)

MICHIGAN STATE UNIV. LIBRARIES
31293007841038